Dealing with large amplitude motion and large size systems with the effective field configuration interaction method

Patrick Cassam-Chenaï, Amine Ilmane

Dealing with large amplitude motion and large size systems with the effective field configuration interaction method

P. Cassam-Chenaï[a)] and A. Ilmane

Université Côte d'Azur, LJAD, UMR 7351, 06100 Nice, France

(Dated: 31 March 2023)

The mean field configuration interaction (MFCI) method is a variational approximation method, which has been developed to solve the Schrödinger equation for molecular vibrations (VMFCI), for electrons (EMFCI), or for both: Electron-Nucleus MFCI. The Rayleigh-Schrödinger perturbation theory generalized to eigen-operators in non-commutative rings has been proposed to solve the Schrödinger equation for molecular rotation-vibration degrees of freedom. These two approaches can be merged in a unified method, the perturbative ansatz at order more than one, giving a more general "effective field" (EF) than the order one "mean field". EF arising from the vibrational motion of semi-rigid molecules have proved useful to compute acurate rotational spectra at moderate computational cost. In the present paper, we argue that EF can also be taken advantage of to deal with systems presenting large amplitude motion such as HOOH and/or a large number of degrees of freedom such as naphtalene.

[a)]Electronic mail: cassam@unice.fr

I. INTRODUCTION

The idea of partitioning the vibrational degrees of freedom (DOF's) of a molecular system and to treat perturbationally the influence of one set onto the other can be traced back to Higgs' early works[1–3]. However, the idea of Higgs has not been pursued at that time. The partitioning of distinguishable DOFs reappeared in a purely variational context: $(J = 0)$-vibrational Hamiltonian were first diagonalized, and then, their eigenfunctions were used to build product basis sets to perform configuration interaction (CI) calculations (or "state interaction"[4]), for the full rovibrational problem[5,6]. This method was often referred to as the "contraction method". It has been further developed by Tennyson and Sutcliffe, who included J-dependent contributions in the vibrational Hamiltonian to treat highly rotationally excited states of floppy molecules[7]. Within a discrete variable representation (DVR) of the angle coordinate of a triatomic molecule, Bačić and Light adapted the contraction method to a purely vibrational context[8]. They inaugurated the "adiabatic contracted method" by using $2D$-sets of distributed Gaussians for the radial DOF's with different dimensions and/or truncations for different angle values, so, the resulting product basis set was not of the direct product type. This adiabatic contraction technique was later combined with Lanczos recursion procedure[9], while Bramley and Carrington proposed the use of "simply contracted basis sets"[10], obtained by diagonalizing reduced-dimension Hamiltonians, the latter being derived from the total Hamiltonian by fixing the value of geometric parameters at equilibrium[10–14]. Further refinements were made by Yu, whose "diabatic contracted" basis for angular coordinates in his two-layer Lanczos algorithm were formed as the lowest eigenstates of a partial Hamiltonian derived by leaving out Coriolis coupling terms, averaging over rotational basis functions, and fixing radial coordinates at two sets of equilibrium reference values, one for the kinetic energy operator and one for the potential energy operator[15].

The mean field configuration interaction (MFCI) method stemmed from the contraction method. It has been developed originally by Cassam-Chenaï and Liévin for molecular vibrations and was called vibrational MFCI (VMFCI)[16–18]. It takes advantage of the contraction technique within a mean-field approach and extends the vibrational self-consistent field (VSCF) approach[19,20] towards a direction pioneered by Bowman and Gasdy[21]. It has proved extremely powerful and flexible to solve the molecular, vibrational, stationary Schrödinger equation[22–24]. In parallel, we have developed a generalized perturbation theory[16,25,26]. The formulas ressemble those obtained from a contact transformation with a standard unitary transformation operator[32]. In addition to the

abundant literature on effective Hamiltonians and contact transformations already cited in our previous works[33–44], we would like to mention the early work of Jorgensen and Pedersen[45] who first exploited the operator decomposition into an even and an odd part to simplify the perturbative expansion algebra. This was further developped by Shavitt[46] with an elegant use of formal series, and recently revisited from a geometric standpoint by Kvaal[47] and Jorgensen[48], with the help of what is sometimes called the"Araki's angles"[49,50] and some subtle condition to extend the treatment to infinite dimensional quasi-degenerate spaces (Appendix B of[48]). However, we will continue to omit the non less abundant literature aiming mainly at building effective ro-vibrational (or rovibronic) Hamiltonian to analyse experiments in the fashion of Shaffer et al.[51]. The specificity of our approach is that it takes explicitly advantage of the tensorial structure of the Hilbert space decomposed into a subsystem Hilbert space times the Hilbert space of the rest of the system: $\mathcal{H} = \mathcal{H}_A \otimes \mathcal{H}_B$. This was pionnered in the case of the partition into vibrational and rotational DOFs by Makushkin and co-workers[40,52–55] and exploited recently in the MIRS code[56] and the NITROGEN code[57], for instance. Such a decomposition should not be confused with the decomposition of the Hilbert space into a direct sum $\mathcal{H} = \mathcal{H}_A \oplus \mathcal{H}_B$ nicely treated by Löwdin[58]. Combined with this perturbation theory, VMFCI solutions give effective rotational observables, from which accurate rotational spectra are calculated[22,59,60]. More recently, this mixed approach has been extended towards quasi-degenerate reference states[61] and non-adiabatic electron-nucleus calculations[62].

In short, the MFCI approach consists in building an effective Hamiltonian for a subset of degrees of freedom (DOF's) called "active", which accounts for the mean field effect of the other DOF's called "spectators", and then to diagonalize this Hamiltonian in a finite basis set. In previous works[59,60,62], we have recognized in the effective Hamiltonian of a MFCI step, a generalized pertubation first order Hamiltonian. So, it was natural to propose a more general method, where one can adjust the order of perturbation to obtain an effective mean-field Hamiltonian of a targeted level of accuracy, assuming that the formal perturbative series of non necessarily commuting, effective operators, converges. The MFCI method is generalized in the sense that the mean-field due to spectator DOF's, used to build the partial Hamiltonian of the active DOF's, can include corrective terms of order greater than one, involving excitations to, or, from the reference spectator state. So, we will talk of "nth-order effective fields" and of the effective field configuration interaction (EFCI) method.

The EFCI method has increased flexibility, since not only one can build any hierarchy

of DOF's partitions (called a "contraction-truncation scheme") as in the MFCI method, but one can also tune up the perturbation order at each MFCI step for each subset of DOF's. In the case of rotational DOF's, GMF of increasing orders due to the vibrational DOF's considered as spectators, give energy levels and wave functions of increasing accuracy as long as there is a significant energy gap between reference and excited spectator states compare to rotational energy differences[61]. The first purpose of the present study is to show that the same holds true for other DOF's types than rotational. Natural candidates are large amplitude motion DOF's whose energy level differences are expected to be orders of magnitude smaller than those of the small amplitude motion DOF's.

So far, GMF have only been used in the final step of a contraction-truncation scheme. In fact, when using GMF at an intermediate step, the method is no longer variational. So, there is no guaranty that iterating the same partition of the DOF's will converge to an self-consistent solution. However, partial GMFCI eigenfunctions are expected to be of better quality than MFCI ones, so that basis sets for use in the next calculation step formed as a direct product of such functions, could be truncated more drastically without loss of accuracy. The second goal of this study is to assess how important this reduction can be at an intermediate step of a contraction-truncation scheme.

In addition to those already mentioned, many methods to solve the molecular rovibrational problem, can be related to the MFCI or GMFCI approaches. So, the short review that follows will not be exhaustive and will focus on works not sufficiently discussed in our previous papers. Let us start by mentioning the partially separated VSCF method of Wright and Gerber which contracts from the start (i.e. not at a chosen step in a hierarchy of partitions as in MFCI), groups of two or three DOF's while limiting the potential to pairwise interactions with inclusion of only a few triplewise coupling terms[63]. Sergeev and Goodson also generalized the VSCF approach to groups of DOF's (see Eq.(9) and paragraph above in[64]). However, in contrast with the GMF approach, their perturbation theory uses the harmonic reference and coupling terms are ordered with respect to the total power in the normal coordinate expansion of the Hamiltonian within the generalized SCF procedure. More recently, the vibrational active space self-consistent field (VASSCF) ansatz proposed by Mizukami and Tew[65] can be viewed VSCFCI (VMFCI iterated up to self-consistency) for a partition where the so-called "bath" DOF's are kept uncontracted. A precursor work conveying similar ideas to the one developed in this paper and initially designed to deal with large amplitude motion is that of Senent et al.[66]. These authors partition the system into two sets that they treat self-consistently in a process that can also be viewed as an VSCFCI calculation.

Then, on the top of that, they add perturbative corrections up to fourth order. Note that DOF's partitioning is different from configuration space partitioning[67]. However the later can also be used to improve the diagonalization efficiency of the CI matrices appearing in GMFCI calculations. Compared to adiabatic methods that have been developed for either floppy systems[8,68] or rotational DOF's[69,70], the GMFCI method is simpler in the sense that only one reduced-dimension Hamiltonian diagonalization is required where many (in fact, as many as the number of inactive DOF grid points) need to be performed in adiabatic approaches, (even if they may be trivial in the case of the harmonic adiabatic approximation of Lauvergnat et al.[71,72]). Furthermore the part played by active or slow DOF's and inactive or fast DOF's is dissymmetrical in the adiabatic approaches, whereas it can be symmetrical or not, depending on the choice of GMF order in the GMFCI method, because the active and inactive (i.e. spectator) DOF's exchange their parts in turn. The GMFCI approach can be seen as a variational approach to treat an Hamiltonian of pertubational origin. A dual approach which consists in starting from perturbation theory and to treat variationally the tightly coupled states has also been implemented in computer codes and proved successful in dealing with medium-to-large molecular systems[73–76]. Other hybrid variation-perturbation methods for solving the nuclear motion problem have appeared recently. Fábri et al. have proposed to treat the Coriolis coupling terms of the Eckart-Watson kinetic energy operator perturbationally on the top of a variational calculation[77]. Their algorithm has been implemented in the code DEWE[78]. Pavlyuchko et al.[79] in the code ANGMOL use approximate vibrational quantum number differences to partition the CI matrix, discard coupling elements when these differences are very large, and compute a second order pertubative correction to diagonal elements of the zero order blocks when the difference is less important. Of course, this relies on the quantum numbers being reasonably good approximate ones. A similar technique is employed when rotations are considered: the coupling between states having different vibrational quantum numbers are treated by a second order-like pertubative correction which can cope with degeneracy or quasi-degeneracy between of zero order diagonal values. The difference with respect to the purely vibrational case is that both the diagonal and off-diagonal Hamiltonian elements of order-zero blocks are corrected. Let us mention also the idea of using perturbative formula to select the important configurations to include in a VCI[23,80–84] in a manner reminiscent of the CIPSI algorithm for electronic calculations[85]. Another, promising basis set compression technique is the so-called "vibrational subspace" approach of Rey et al.[86,87].

The article is organized as follows: We begin with a presentation of the main ideas

and equations, the GMFCI method is based upon. Then, we consider the HOOH system and study different contraction schemes with or without rotational DOFs in conjonction with different mean field orders. We conclude on the accuracy that can be achieved and the prospect of using high order mean field for system with large amplitude motion.

II. THE GMFCI METHOD

A natural approximation strategy in physics, which follows Descartes second precept, consists in separating the system degrees of freedom into subgroups. In quantum physics, this translates in building the state space as a tensor product of DOF subgroup Hilbert spaces. However, physical wave functions are seldom exactly decomposable into a simple tensor product of factors pertaining to the different Hilbert subspaces, even when one disregards spin statistics or EPR correlations.

The MFCI method has been proposed to separate DOF and contract wave functions, according to a hierarchy of DOF partitions, designed to capture the physics of the system while controling computational costs. More precisely, the MFCI method consists in performing configuration interactions (CI) of some DOF in the mean field of the others. The sizes of the finite basis sets used in successive CI, is kept within a manageable range, owing to a basis "truncation scheme" associated to the DOF partitioning or "contraction scheme". The power of the method comes from the mean field (MF) term added to the reduced-dimension Hamiltonians. In the GMFCI method, the expression of this MF term is extented to include corrective terms according to a pertubative expansion.

A. Partitions of DOF

Consider a quantum system with N distinguishable DOF. A GMFCI step starts with a partition, P, of the N DOF into n_P subsets :

$$P = (I_1, I_2, \cdots, I_{n_P}) = (\{i_1^1, i_2^1, \cdots, i_{k_1}^1\}, \{i_1^2, i_2^2, \cdots, i_{k_2}^2\}, \cdots, \{i_1^{n_P}, i_2^{n_P}, \cdots, i_{k_{n_P}}^{n_P}\}) \quad (1)$$

for which the Hamiltonian can be written as:

$$\begin{aligned} H = h_0 &+ \sum_{\gamma_1=1}^{n_P} h_{\gamma_1}(I_{\gamma_1}) \\ &+ \sum_{1\le\gamma_1<\gamma_2\le n_P} h_{\gamma_1,\gamma_2}(I_{\gamma_1}) h_{\gamma_1,\gamma_2}(I_{\gamma_2}) \\ &+ \cdots + h_{1,2,\cdots,n_P}(I_1) h_{1,2,\cdots,n_P}(I_2) \cdots h_{1,2,\cdots,n_P}(I_{n_P}), \end{aligned} \quad (2)$$

where $h_{\gamma_1,\gamma_2,...,\gamma_k}(I_{\gamma_l})$ denotes an operator acting on DOF in subsets I_{γ_l}. In principle, H can always be decomposed formally in this way, however, the summations may be infinite. Such a decomposition is not necessary to implement the GMFCI idea, as shown in[62], but it makes several steps in the implementation of the method computationnally cheaper.

Then, one defines an equal or coarser partition, $Q = (J_1, J_2, \cdots, J_{n_Q})$, satisfying $n_Q \leq n_P$ and $\forall\gamma \in \{1, \cdots, n_P\}, \exists\alpha \in \{1, \cdots, n_Q\}$ such that $I_\gamma \subseteq J_\alpha$. For the GMFCI step under consideration, we call "contractions" the subsets J_α, and "components of contraction J_α" the subsets I_γ such that $I_\gamma \subseteq J_\alpha$. When successive GMFCI steps are performed, the *components* of one step are the *contractions* of the previous step.

B. Product basis sets

Let us assume that contraction J_α has β_α components :

$$\begin{aligned} J_\alpha &= I_{\gamma_1} \cup I_{\gamma_2} \cup \cdots \cup I_{\gamma_{\beta_\alpha}} \\ &= \left\{ i_1^{\gamma_1}, \cdots, i_{k_{\gamma_1}}^{\gamma_1}, \cdots, i_1^{\gamma_{\beta_\alpha}}, \cdots, i_{k_{\gamma_{\beta_\alpha}}}^{\gamma_{\beta_\alpha}} \right\} \\ &= \left\{ j_1^\alpha, \cdots, j_{l_\alpha}^\alpha \right\} \quad \text{with} \quad l_\alpha = k_{\gamma_1} + \cdots + k_{\gamma_{\beta_\alpha}}. \end{aligned} \tag{3}$$

For each component I_γ, we suppose that we have a basis set of orthonormalized functions, $\{\phi_{I_\gamma}^{m_\gamma}\}_{m_\gamma \in \{0,...,d_\gamma\}}$, spanning an Hilbert subspace of dimension $(d_\gamma + 1)$. We further assume that these functions are eigenfunctions of some model Hamiltonian, H_γ^{mod}, associated to the eigenvalues, $\{E_{I_\gamma}^{m_\gamma}\}_{m_\gamma \in \{0,...,d_\gamma\}}$, in increasing order, the indice $m_\gamma = 0$ corresponding to the ground state of H_γ^{mod}.

For contraction J_α, we build a so-called "product basis set", $\{\Phi_{J_\alpha}^{M_\alpha}\}_{M_\alpha}$, spanning an Hilbert subspace of dimension say, D_α, by constructing product functions of the form:

$$\Phi_{J_\alpha}^{M_\alpha} = \bigotimes_{I_\gamma \subseteq J_\alpha} \phi_{I_\gamma}^{m_\gamma} \tag{4}$$

or more explicitly, writing variable dependencies:

$$\Phi_{J_\alpha}^{M_\alpha}(q_{j_1^\alpha}, \cdots, q_{j_{l_\alpha}^\alpha}) = \prod_{I_\gamma \subseteq J_\alpha} \phi_{I_\gamma}^{m_\gamma}(q_{i_1^\gamma}, \cdots, q_{i_{k_\gamma}^\gamma}),$$

where $M_\alpha = (m_{\gamma_1}, \cdots, m_{\gamma_{\beta_\alpha}})$, is the multiplet of the indices "m_γ", appearing on the right-hand side of the equation. So, $M_\alpha = (0, ..., 0)$, will correspond to the product of ground state functions.

The dimension, D_α, of the basis set for contraction J_α can be different from the product of dimensions of its component's basis sets, $\prod_{I_\gamma \subseteq J_\alpha} (d_\gamma + 1)$, because of possible basis function truncations, performed according to a set of energy criteria (indexed by j) of the form,

$$\sum_{I_\gamma \subseteq J_\alpha} \lambda^j_{I_\gamma} E^{m_\gamma}_{I_\gamma} < E^j_{J_\alpha}. \tag{5}$$

The $E^{m_\gamma}_{I_\gamma}$'s are the energies of the components of the product functions $\Phi^{(m_{\gamma_1},\cdots,m_{\gamma_{\beta_\alpha}})}_{J_\alpha}$, the $\lambda^j_{I_\gamma}$'s are positif real numbers, and the $E^j_{J_\alpha}$'s are energy cutoff thresholds. Typically, we choose $\lambda^j_{I_\gamma} = 1$ for all I_γ or, $\lambda^j_{I_\gamma} = 0$ for all I_γ but one, and the $E^j_{J_\alpha}$'s within gaps of the contraction or its components spectra.

C. Mean field Hamiltonian

Now, we consider a given contraction J_α as "active", and call the other contractions "spectators". For the active contraction J_α, we define a partial Hamiltonian, H_α, by grouping all the terms in H involving the DOF in components I_γ of J_α:

$$\begin{aligned} H_\alpha = h_0 + \sum_{\substack{\gamma_1 \\ such\ that \\ I_{\gamma_1} \subseteq J_\alpha}} h_{\gamma_1}(I_{\gamma_1}) + \sum_{\substack{\gamma_1 < \gamma_2 \\ such\ that \\ I_{\gamma_1}, I_{\gamma_2} \subseteq J_\alpha}} h_{\gamma_1,\gamma_2}(I_{\gamma_1}) h_{\gamma_1,\gamma_2}(I_{\gamma_2}) \\ + \cdots + \sum_{\substack{\gamma_1 < \cdots < \gamma_{\beta_\alpha} \\ such\ that \\ I_{\gamma_1},\cdots,I_{\gamma_{\beta_\alpha}} \subseteq J_\alpha}} h_{\gamma_1,\cdots,\gamma_{\beta_\alpha}}(I_{\gamma_1}) \cdots h_{\gamma_1,\cdots,\gamma_{\beta_\alpha}}(I_{\gamma_{\beta_\alpha}}) \end{aligned} \tag{6}$$

Then we consider an eigenvalue equation for J_α:

$$[H^{eff}_\alpha - \epsilon_\alpha]\Phi_\alpha = 0, \tag{7}$$

where H^{eff}_α is an "effective" Hamiltonian determined according to perturbative expressions:

Order 0: Simple contraction method Hamiltonian

$$H^{eff}_\alpha = H_\alpha \tag{8}$$

Order 1: MFCI Hamiltonian[16–18]

$$H^{eff}_\alpha = H_\alpha + \langle \bigotimes_{I_\gamma \not\subseteq J_\alpha} \phi^{m^0_\gamma}_{I_\gamma} | H - H_\alpha | \bigotimes_{I_\gamma \not\subseteq J_\alpha} \phi^{m^0_\gamma}_{I_\gamma} \rangle \tag{9}$$

Order 2: second order GMFCI Hamiltonian

$$H_\alpha^{eff} = H_\alpha + \langle \bigotimes_{I_\gamma \not\subset J_\alpha} \phi_{I_\gamma}^{m_\gamma^0} | H - H_\alpha | \bigotimes_{I_\gamma \not\subset J_\alpha} \phi_{I_\gamma}^{m_\gamma^0} \rangle$$

$$+ \sum_{\substack{(m_{\gamma_1},\cdots,m_{\gamma_{(n_P-\beta_\alpha)}}) \neq (m^0_{\gamma_1},\cdots,m^0_{\gamma_{(n_P-\beta_\alpha)}}) \\ for\ \gamma_1,\ldots,\gamma_{(n_P-\beta_\alpha)}\ such\ that\ I_{\gamma_l} \not\subset J_\alpha}} \frac{\langle \bigotimes_{I_\gamma \not\subset J_\alpha} \phi_{I_\gamma}^{m_\gamma^0} | H - H_\alpha | \bigotimes_{I_\gamma \not\subset J_\alpha} \phi_{I_\gamma}^{m_\gamma} \rangle \langle \bigotimes_{I_\gamma \not\subset J_\alpha} \phi_{I_\gamma}^{m_\gamma} | H - H_\alpha | \bigotimes_{I_\gamma \not\subset J_\alpha} \phi_{I_\gamma}^{m_\gamma^0} \rangle}{\sum_{\gamma \ / \ I_\gamma \not\subset J_\alpha} E_{I_\gamma}^{m_\gamma^0} - E_{I_\gamma}^{m_\gamma}}, \tag{10}$$

and so on, up to an arbitrary order, for a non-degenerate reference spectator product function associated to indices $(m^0_{\gamma_1}, \cdots, m^0_{\gamma_{(n_P-\beta_\alpha)}})$. These expressions are those given by the generalized perturbation theory of Refs. ([25,26,59]). They can also be derived through equivalent approaches[32,38–40]. Dirac bracket notation corresponds in these equations to integration over spectator variables only.

The summation on the m_γ's in Eq. (10) can be restricted according to constraints of the types given in expression (5). Note that, the mean field corrective terms correspond, here, to mean field effects of the approximate ground states of the spectator modes $(m^0_{\gamma_1}, \cdots, m^0_{\gamma_{(n_P-\beta_\alpha)}}) = (0, \cdots, 0)$. As explained in[18], it is not suitable to use an excited state mean field, (and it holds as well for an excited state generalized mean field), if one intends to perform further GMFCI steps. In contrast, at the last step of a sequence of GMFCI calculations, one can modify the equations above to use a generalized mean field corresponding to an arbitrary spectator state. This is straightforward if the spectator approximate, reference state is non degenerate, that is to say, if it can be represented by $\bigotimes_{I_\gamma \not\subset J_\alpha} \phi_{I_\gamma}^{m_\gamma^0}$ and if this is the only product function of this type with approximate energy equal to $\sum_{\gamma \ / \ I_\gamma \not\subset J_\alpha} E_{I_\gamma}^{m_\gamma^0}$. It suffices to replace the "0" superscripts by the "m_γ^0" of the reference state, and to avoid the multiplet, $(m^0_{\gamma_1}, \cdots, m^0_{\gamma_{(n_P-\beta_\alpha)}})$, in the GMFCI Hamiltonian summations over $(m_{\gamma_1}, \cdots, m_{\gamma_{(n_P-\beta_\alpha)}})$. In case of a k-fold degenerate or quasi degenerate excited spectator state, one should use a k-dimensional super-Hamiltonian for the active contraction, as explained elsewhere[61].

A n^{th}-order GMFCI calculation consists in solving the eigen-equation (7) for a n^{th}-order generalized mean field Hamiltonian, by performing a "configuration interaction" in the product basis sets, Eq. (4), that is to say, by diagonalizing the representation of the Hamiltonian in this finite dimensional Hilbert subspace basis (Rayleigh-Ritz method[88]).

Thereby, we obtain for the active contraction a new basis set, $\{\phi_{J_\alpha}^{m_\alpha}\}_{m_\alpha \in \{0,\ldots,d_\alpha\}}$, of

dimension $(d_\alpha + 1)$, made of eigenvectors of the generalized mean field Hamiltonians. So, the process can be iterated, the H_γ^{mod} of step $n+1$ being the H_α^{eff} of step n. The eigenvalues $\{E_{J_\alpha}^{m_\alpha}\}_{m_\alpha \in \{0,\ldots,d_\alpha\}}$ associated to the $\{\phi_{J_\alpha}^{m_\alpha}\}_{m_\alpha \in \{0,\ldots,d_\alpha\}}$ will serve to truncate the product basis sets according to energy criteria (5).

In practice, $(d_\alpha + 1)$ can be less than D_α, as one needs not to calculate all the eigenpairs of H_α^{eff}. This is so, when some high energy states will not be required at all for the construction of the product basis sets of the next step according to the anticipated truncation criteria to be applied.

Note that, in the computer code CONVIV[89], a GMFCI is performed for each contraction of the Q-partition before updating the H_γ^{mod}. That is to say, the n_Q contractions of Q are treated simultaneously as active and the same n_P sets of eigenstates $\{E_{I_\gamma}^{m_\gamma}, \phi_{I_\gamma}^{m_\gamma}\}_{m_\gamma \in \{0,\ldots,d_\gamma\}}$ are used to build the spectator product functions appearing in the n_Q GMFCI Hamiltonians. However, the orders of the n_Q GMFCI Hamiltonians need not be the same, nor the truncation criteria for the spectator basis functions. Then, the n_Q new sets of eigenstates, $\{E_{J_\alpha}^{m_\alpha}, \phi_{J_\alpha}^{m_\alpha}\}_{m_\alpha \in \{0,\ldots,d_\alpha\}}$, are used to update the n_P sets, $\{E_{I_\gamma}^{m_\gamma}, \phi_{I_\gamma}^{m_\gamma}\}_{m_\gamma \in \{0,\ldots,d_\gamma\}}$. In other words, CONVIV performs n_Q GMFCI steps in parallel for each successive partition, instead of sequential GMFCI steps. This parallel treatment has been found more effective for vibrational MFCI calculations, whereas this is not the case for electronic MFCI[18].

D. Calculation of observables

Whether one performs sequential or parallel GMFCI steps, after each step, one has to decide whether the Q-partition is sufficient, or if further contractions are necessary, to capture properly the important physical couplings between DOF's. If eventually, all the DOF's are contracted and $Q = (\{1, 2, \cdots, N\})$, then the eigenfunctions obtained can be used to calculate in the standard way, observable expectation values or transition matrix elements for the full system. In contrast, if, at the last step, Q still contains more than one contraction, there are different ways to compute properties just as there are different orders to compute the effective Hamiltonian.

The eigenvalues of the effective Hamiltonian of each contraction can be interpreted as energy levels of the subsystems corresponding to the DOF pertaining to the contraction. Assuming that the observable, O, can be expanded in the same fashion as the

Hamiltonian, Eq.(2),

$$O = o_0 + \sum_{\alpha_1=1}^{n_Q} o_{\alpha_1}(J_{\alpha_1}) + \sum_{1\le\alpha_1<\alpha_2\le n_Q} o_{\alpha_1,\alpha_2}(J_{\alpha_1})o_{\alpha_1,\alpha_2}(J_{\alpha_2}) + \cdots + o_{1,2,\cdots,n_Q}(J_1)o_{1,2,\cdots,n_Q}(J_2)\cdots o_{1,2,\cdots,n_Q}(J_{n_Q}), \quad (11)$$

it is tempting to compute its matrix element between two total states represented by the product functions, $\bigotimes_{\alpha\in\{1,\ldots,n_Q\}} \phi_{J_\alpha}^{m_\alpha}$ and $\bigotimes_{\alpha\in\{1,\ldots,n_Q\}} \phi_{J_\alpha}^{m'_\alpha}$ according to the following equation,

$$\begin{aligned}
&\langle \bigotimes_{\alpha\in\{1,\ldots,n_Q\}} \phi_{J_\alpha}^{m_\alpha} | O | \bigotimes_{\alpha\in\{1,\ldots,n_Q\}} \phi_{J_\alpha}^{m'_\alpha} \rangle = \\
&o_0 \prod_{\alpha\in\{1,\ldots,n_Q\}} \delta_{m_\alpha m'_\alpha} + \sum_{\alpha_1=1}^{n_Q} \langle \phi_{J_{\alpha_1}}^{m_{\alpha_1}} | o_{\alpha_1}(J_{\alpha_1}) | \phi_{J_{\alpha_1}}^{m'_{\alpha_1}} \rangle \prod_{\alpha\in\{1,\ldots,n_Q\}\setminus\{\alpha_1\}} \delta_{m_\alpha m'_\alpha} \\
&+ \sum_{1\le\alpha_1<\alpha_2\le n_Q} \langle \phi_{J_{\alpha_1}}^{m_{\alpha_1}} | o_{\alpha_1,\alpha_2}(J_{\alpha_1}) | \phi_{J_{\alpha_1}}^{m'_{\alpha_1}} \rangle \langle \phi_{J_{\alpha_2}}^{m_{\alpha_2}} | o_{\alpha_1,\alpha_2}(J_{\alpha_2}) | \phi_{J_{\alpha_2}}^{m'_{\alpha_2}} \rangle \prod_{\alpha\in\{1,\ldots,n_Q\}\setminus\{\alpha_1,\alpha_2\}} \delta_{m_\alpha m'_\alpha} \\
&+ \cdots + \prod_{\alpha\in\{1,\ldots,n_Q\}} \langle \phi_{J_\alpha}^{m_\alpha} | o_{1,2,\cdots,n_Q}(J_\alpha) | \phi_{J_\alpha}^{m'_\alpha} \rangle, \quad (12)
\end{aligned}$$

in particular, the expectation value over $\bigotimes_{\alpha\in\{1,\ldots,n_Q\}} \phi_{J_\alpha}^{m_\alpha}$ would be,

$$\begin{aligned}
&\langle \bigotimes_{\alpha\in\{1,\ldots,n_Q\}} \phi_{J_\alpha}^{m_\alpha} | O | \bigotimes_{\alpha\in\{1,\ldots,n_Q\}} \phi_{J_\alpha}^{m_\alpha} \rangle = o_0 + \sum_{\alpha_1=1}^{n_Q} \langle \phi_{J_{\alpha_1}}^{m_{\alpha_1}} | o_{\alpha_1}(J_{\alpha_1}) | \phi_{J_{\alpha_1}}^{m_{\alpha_1}} \rangle \\
&+ \sum_{1\le\alpha_1<\alpha_2\le n_Q} \langle \phi_{J_{\alpha_1}}^{m_{\alpha_1}} | o_{\alpha_1,\alpha_2}(J_{\alpha_1}) | \phi_{J_{\alpha_1}}^{m_{\alpha_1}} \rangle \langle \phi_{J_{\alpha_2}}^{m_{\alpha_2}} | o_{\alpha_1,\alpha_2}(J_{\alpha_2}) | \phi_{J_{\alpha_2}}^{m_{\alpha_2}} \rangle \\
&+ \cdots + \prod_{\alpha\in\{1,\ldots,n_Q\}} \langle \phi_{J_\alpha}^{m_\alpha} | o_{1,2,\cdots,n_Q}(J_\alpha) | \phi_{J_\alpha}^{m_\alpha} \rangle. \quad (13)
\end{aligned}$$

However, this is not necessarily consistent with the derivation of the $\phi_{J_\alpha}^{m_\alpha}$'s if some of the latter correspond to an order 2 GMF, or, to an order 1 MF for a spectator reference state different from its counterpart in $\bigotimes_{\alpha\in\{1,\ldots,n_Q\}} \phi_{J_\alpha}^{m_\alpha}$ or $\bigotimes_{\alpha\in\{1,\ldots,n_Q\}} \phi_{J_\alpha}^{m'_\alpha}$.

A more rigorous expression can be derived when $(m_1,\cdots,m_{n_Q})$ and $(m'_1,\cdots,m'_{n_Q})$ differ by at most one component, say, without loss of generality, their first component. That is to say, $\forall\alpha\in\{2,\ldots,n_Q\}, m_\alpha = m'_\alpha$, and, we denote by, m^0_α, this common value. (In fact, if this condition is not met, further contractions should be made to achieve it and avoid using Eqs.(12) and (13) as such.) So, let us assume that the last GMFCI step corresponds to contraction 1 being active, with a spectator reference state equal to the product function $\bigotimes_{\alpha\in\{2,\ldots,n_Q\}} \phi_{J_\alpha}^{m^0_\alpha}$. The effective Hamiltonians of section II C are related to effective wave operators, as described in[25]. For example, Eq.(10), generalized

for the spectator reference state, $(m_2^0, \cdots, m_{n_Q}^0)$, is related to a first order effective wave operator, acting on J_1-states, of the form,

$$\hat{\phi}_{J_1}^{eff} = Id_{J_1} \otimes \phi_{J_2}^{m_2^0} \otimes \cdots \otimes \phi_{J_{n_Q}}^{m_{n_Q}^0}$$

$$+ \sum_{(m_2,\cdots,m_{n_Q}) \neq (m_2^0,\cdots,m_{n_Q}^0)} \frac{\langle \bigotimes_{\alpha=2}^{n_Q} \phi_{J_\alpha}^{m_\alpha} | H - H_{J_1} | \bigotimes_{\alpha=2}^{n_Q} \phi_{J_\alpha}^{m_\alpha^0} \rangle}{\sum_{\alpha=2}^{n_Q} E_{J_\alpha}^{m_\alpha^0} - E_{J_\alpha}^{m_\alpha}} \otimes \phi_{J_2}^{m_2} \otimes \cdots \otimes \phi_{J_{n_Q}}^{m_{n_Q}}, \quad (14)$$

where Id_{J_1} denotes the identity operator on J_1-wave functions. Then, the matrix element of observable, O of Eq.(11), between two total states represented by the multiplets $(m_1, m_2^0, \cdots, m_{n_Q}^0)$ and $(m_1', m_2^0, \cdots, m_{n_Q}^0)$ is, up to order 1 in the wave operator expansion,

$$\langle \phi_{J_1}^{m_1} \ \hat{\phi}_{J_1}^{eff\,\dagger} | O | \hat{\phi}_{J_1}^{eff} \phi_{J_1}^{m_1'} \rangle = \langle \phi_{J_1}^{m_1} \otimes \phi_{J_2}^{m_2^0} \otimes \cdots \otimes \phi_{J_{n_Q}}^{m_{n_Q}^0} | O | \phi_{J_1}^{m_1'} \otimes \phi_{J_2}^{m_2^0} \otimes \cdots \otimes \phi_{J_{n_Q}}^{m_{n_Q}^0} \rangle$$

$$+ \sum_{(m_2,\cdots,m_{n_Q}) \neq (m_2^0,\cdots,m_{n_Q}^0)} \Bigg(\langle \phi_{J_1}^{m_1} \otimes \phi_{J_2}^{m_2^0} \otimes \cdots \otimes \phi_{J_{n_Q}}^{m_{n_Q}^0} | O | \frac{\langle \bigotimes_{\alpha=2}^{n_Q} \phi_{J_\alpha}^{m_\alpha} | H - H_{J_1} | \bigotimes_{\alpha=2}^{n_Q} \phi_{J_\alpha}^{m_\alpha^0} \rangle \phi_{J_1}^{m_1'}}{\sum_{\alpha=2}^{n_Q} E_{J_\alpha}^{m_\alpha^0} - E_{J_\alpha}^{m_\alpha}} \otimes \phi_{J_2}^{m_2} \otimes \cdots \otimes \phi_{J_{n_Q}}^{m_{n_Q}} \rangle$$

$$+ \langle \frac{\phi_{J_1}^{m_1} \langle \bigotimes_{\alpha=2}^{n_Q} \phi_{J_\alpha}^{m_\alpha} | H - H_{J_1} | \bigotimes_{\alpha=2}^{n_Q} \phi_{J_\alpha}^{m_\alpha^0} \rangle^\dagger}{\sum_{\alpha=2}^{n_Q} E_{J_\alpha}^{m_\alpha^0} - E_{J_\alpha}^{m_\alpha}} \otimes \phi_{J_2}^{m_2} \otimes \cdots \otimes \phi_{J_{n_Q}}^{m_{n_Q}} | O | \phi_{J_1}^{m_1'} \otimes \phi_{J_2}^{m_2^0} \otimes \cdots \otimes \phi_{J_{n_Q}}^{m_{n_Q}^0} \rangle \Bigg) \quad (15)$$

where $\hat{\phi}_{J_1}^{eff\,\dagger}$, (respectively, $\langle \Psi | H - H_{J_1} | \Psi' \rangle^\dagger$), is the Hermitian conjugate of $\hat{\phi}_{J_1}^{eff}$, (respectively, $\langle \Psi | H - H_{J_1} | \Psi' \rangle$) acting on the left on J_1-wave functions. Note that each term in the left-hand side of Eq. (15) is of the form of the right-hand side of Eq. (12), so, it can be expanded according to this equation. If observable O, itself, is expressed as a perturbative series, then the terms retained in the expansion must be determined according to the required, total, expansion order. Just like for the Hamiltonian, the summation on components 2 to n_Q basis functions can be truncated according to energy criteria, Eqs. (5).

III. INTERNAL MOTION SPECTRUM OF H_2O_2, A CASE STUDY

The theory outlined in the previous section, originally developed for the computation of rotation-vibration spectra of molecules, is directly applicable to any quantum system with distinguishable degrees of freedom. This theory is more general than what we have used in previous applications, since a GMF can be used at any step of a MFCI calculation, for any contraction. The calculation of the rotational spectra of methane in[59] was a particular case of GMFCI with a GMF of order more than 1 (up to 4), performed solely at the final step.

To study the use of GMF at intermediate contraction steps, we have chosen the case example of the hydrogen peroxyde molecule. This system is often used as a benchmark

for assessing new theoretical developments[12,90–100], for it is one of the simplest molecule with a large amplitude DOF. We report hereforth the details of our calculations for this case study.

A. Potential Energy Surface of H_2O_2

We used the CCSD(T)-F12b/aug-cc-pV**5**Z adiabatic Potential Energy Surface (PES) of Malyszek and Koput[108], whose coefficients and geometry parameters are provided as supporting information with this reference. The PES includes corrections accounting for core-electron correlations, second-order Douglas-Kroll-Hess (DKH2) scalar relativistic contributions, higher-order valence-electron correlation, and diagonal Born-Oppenheimer (BO) non-adiabatic contributions. Note that, in addition, the equilibrium parameters, before corrections, were averaged over CCSD(T)-F12b/aug-cc-pV**5**Z and CCSD(T)/aug-cc-pV**7**Z results to approach the complete basis set (CBS) limit.

The potential is expanded in the form:

$$V(q_1, q_2, q_3, q_4, q_5, \varphi) = \sum_{ijklmn} c_{ijklmn} q_1^i q_2^j q_3^k q_4^l q_5^m \cos(n\varphi)$$

where

- q_1, q_2 and q_3 are SPF coordinates[107] corresponding resp. to r_1, r_2 and R in Fig.1;
- $q_4 = (\theta_1 - \theta_1^0)$ and $q_5 = (\theta_2 - \theta_2^0)$ where θ_1^0 and θ_2^0 are the angles in the reference geometry;
- φ is the torsional angle.

The global minimum (in the physically relevant domain) of the fitted PES was found to be at -0.474 cm^{-1} with geometric parameters ($\varphi^{min} = 113.189°$, $R^{min} = 2.742$ Bohr, $r_1^{min} = r_2^{min} = 1.819$ Bohr, $\theta_1^{min} = \theta_2^{min} = 100.025°$). The values of R^{min} , r_1^{min}, and θ_1^{min} differ slightly from those of the reference parameters given in supporting information of Ref.[108]. We considered the shift small enough to keep unchanged the original form of the Malyszek and Koput PES. Figure 6 in Appendix A displays 1D-sections of this PES. It shows the finite barriers which were taken into account to chose the modal basis sets: since the PES is not bounded from below, care must be taken to avoid basis functions with a too large extension in the unbounded region[18].

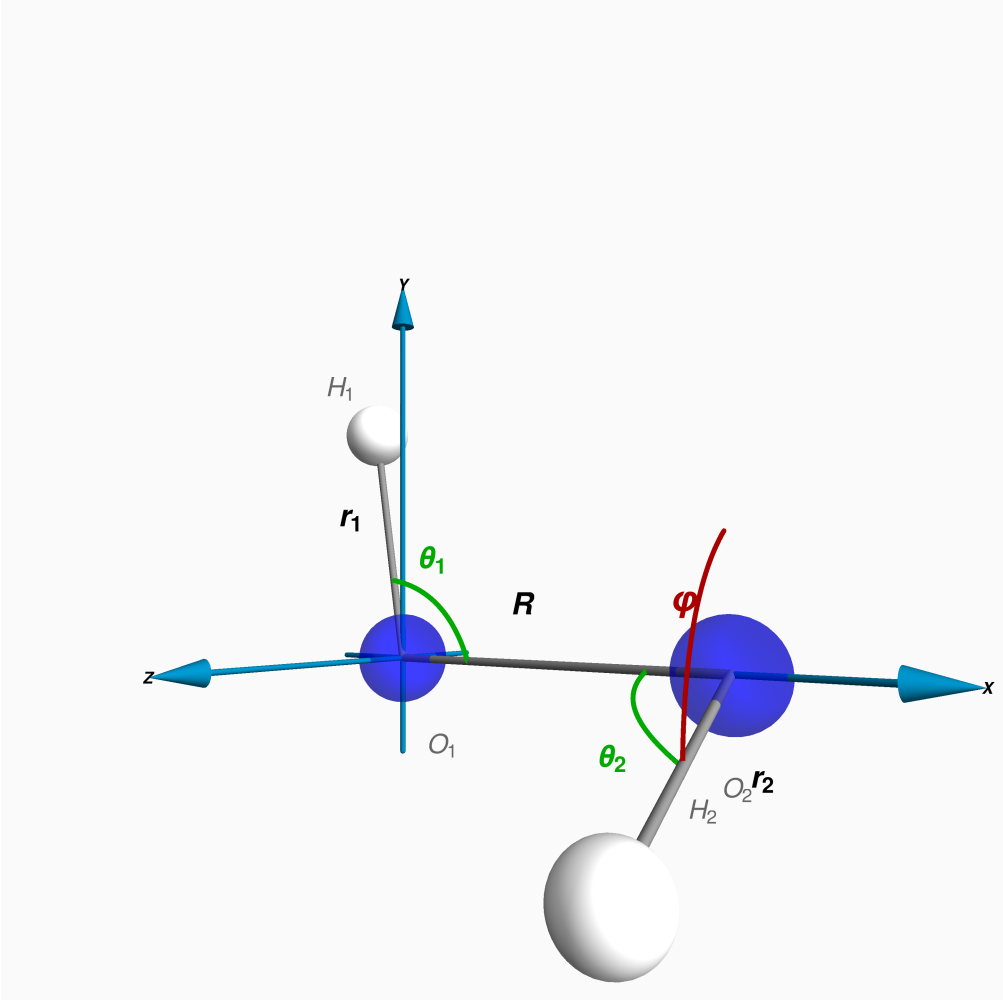

FIG. 1. Geometrical parameters of HOOH.

B. Kinetic Energy Operator for H_2O_2

We have followed the formulas of Lauvergnat and Nauts[103], with the help of the MATHEMATICA symbolic algebra package[128], to derive the Kinetic Energy Operator (KEO) of H_2O_2 in the valence coordinates of Fig. 1.

Les mouvements de pliage font apparaître dans l'opérateur cinétique des termes faisant intervenir $cos(\theta)$, $sin(\theta)$,$tg(\theta)$, $cotg(\theta)$, $cosc(\theta)$. Ces dernières peuvent être intégrées analytiquement dans une base Pöschl-Teller trigonométrique. Ces intégrales sont implémentées dans le code CONVIV. Mais cette partie du code est bridée pour l'instant car une modification importante du code CONVIV serait nécessaire pour les introduire (changement du codage interne des intégrales) si tant est qu'on puisse les obtenir, nous avons préféré nous focaliser sur d'autres aspects.

Pour passer outre cette difficulté nous avons développé en série les termes faisant intervenir les variables θ_1 et θ_2. Ce choix se justifie d'un point de vue conceptuel par

le fait que ces mouvements ont de petites amplitudes. Cet argument est complété par l'étude récente de Strobusch and al.[109,110] sur la convergence du spectre de HOOH en fonction de l'ordre de développement en coordonnées curvilignes. Cette étude affirme qu'à partir de l'ordre deux le spectre est suffisamment convergé.

Dans l'étude de Strobusch et al., l'opérateur cinétique a été développé en série sur les six variables internes que compte le système. Dans notre étude nous avons développé en série que sur deux des six variables. En d'autres termes, un traitement exact de l'opérateur cinétique est effectué sur quatre des coordonnées. A terme un traitement exact de tout l'opérateur sera considéré.

C. Contracted basis sets for H_2O_2

Les paramètres de la base ont été choisis de telle sorte que le décalage q_0 coïncide avec la configuration de référence de la SEP et que la fréquence fondamentale de la base soit à peu près égale à celle du mode.

Toutefois un problème inattendu s'est présenté lors du choix des paramètres de la base pour les mouvements de pliage. Les intégrales du code CONVIV sont implémentées de telle sorte à ce qu'elles soient les plus générales possibles. Pour cela la normalisation de Wilson ainsi qu'un facteur d'échelle sont utilisés. La normalisation de Wilson permet de s'affranchir de l'élément de volume qui dépend des coordonnées et, le facteur d'échelle permet d'utiliser des variables pondérées ou non par la masse. Telles que les formules sont définies, il est nécessaire de connaître les masses réduites lorsque des variables non-pondérées par les masses sont utilisées.

Le calcul de la masse réduite n'est généralement pas compliqué, il s'agit de la moitié de l'inverse du coefficient constant du terme P^2 ($\frac{1}{2m_{\text{réduite}}}P^2$). Etant donné notre choix de ne développer en série que par rapport à deux variables, une des conséquences a été la non existence d'un terme constant devant les opérateurs $P^2_{\theta_1}$ et $P^2_{\theta_2}$ ce qui pose un problème car nous avons utilisé la masse réduite comme facteur d'échelle afin de redéfinir les paramètres de la base ce qui a permis la généralisation du calcul des intégrales en coordonnées autres que les coordonnées normales. Dans ce cas il peut être utile d'utiliser le critère de maximum de projection afin de fixer les bons paramètres de la base.

Dans la table sont résumés les différents paramètres utilisés pour le calcul du spectre vibrationnel. On peut observer que la fréquence de la base harmonique est très grande.

Cette valeur est toute à fait normale car la pondération par la masse a été prise en compte à ce niveau.

Mode	Type	Dimension	Paramètres de la base
$I_1 = \{\nu_4\}$	Chebyshev	$C_{30}^1 = \mathbf{30}$	–
$I_2 = \{\nu_3\}$	Kratzer	$C_{10}^1 = \mathbf{10}$	$D = 188411.76\ (cm^{-1})$, $q0 = 2.7503\ (au)$
$I_3 = \{\nu_1, \nu_5\}$	Kratzer	$C_{10+2-1}^2 = \mathbf{55}$	$D = 169888.81\ (cm^{-1})$, $q0 = 1.8190\ (au)$
$I_4 = \{\nu_2, \nu_6\}$	Harmonique	$C_{10+2-1}^2 = \mathbf{55}$	$\omega = 7124135.045\ (cm^{-1})$, $q0 = 0\ (au)$

TABLE I. Paramètres de la base modale.

Dans la méthode ICCE, le principe général à respecter lors du choix des contractions est de mettre ensemble les modes qui sont fortement couplés. Dans ce cas, les énergies de chaque mode après contraction seront fortement influencées. Comme il a été mis en évidence par le passé, l'abaissement de l'énergie de point zéro sera utilisé comme critère de sélection.

La partition initiale des DLs que nous avons utilisés :

$$P = (I_1, I_2, I_3, I_4) = (\{\nu_4\}, \{\nu_3\}, \{\nu_1, \nu_5\}, \{\nu_2, \nu_6\}) = (\{\varphi\}, \{q_3\}, \{q_4, q_5\}, \{q_1, q_2\})$$

Le fait de contracter les deux pliages (q_2, q_6) et les deux modes d'élongation (q_1, q_5) permet de respecter la symétrie de l'hamiltonien entre $(r_1, \theta_1) \leftrightarrow (r_2, \theta_2)$.

Le type de base a été choisi selon le type de terme apparaissant dans l'expression de la SEP et de l'opérateur cinétique afin d'avoir des intégrales connues de facon analytique ou exacte par méthodes de quadratures (du moins pour certaines).

Le mouvement de torsion est décrit par une série en $cos(n\theta)$. Ce type de terme s'intégre bien par la méthode de quadrature Gauss-Chebyshev. Les mouvements d'élongation sont décrits par les coordonnées SPF que nous avons développées afin de faire apparaître des termes du type $\frac{1}{q^n}$ dont les intégrales sont connues de facon analytique dans une base de Kratzer. Pour ces deux types de mouvements, on voit apparaître dans l'expression exacte de l'opérateur cinétique les mêmes termes que dans la SEP. Ceci est un point positif car pour ces mouvements aucun développement en série de l'opérateur cinétique ne sera nécessaire et ainsi ils seront traités d'une facon exacte.

Afin de mener cette étude nous avons utilisé un développement à l'ordre trois de l'opérateur cinétique, le jugeant suffisamment convergé. Nous avons réalisé, par la suite, différents calculs et pour différents schémas de contraction. Nous n'avons considéré que les contractions binaires car le but est de déterminer les modes fortement couplés.

Nous avons commencé notre calcul en effectuant neuf itérations VMFCI (voir figure 2) sans aucune troncature de la base. Ceci permet d'avoir des états bien convergés pour l'étude des contractions à réaliser par la suite. Ici nous substituons aux coordonnées q_i une notation en fonction des modes de vibration suivant les conventions spectroscopiques.

Dans la suite on notera les contractions de la partition initiale par des chiffres de 1 à 4, i.e. $P = (I_1, I_2, I_3, I_4) = (1, 2, 3, 4)$.

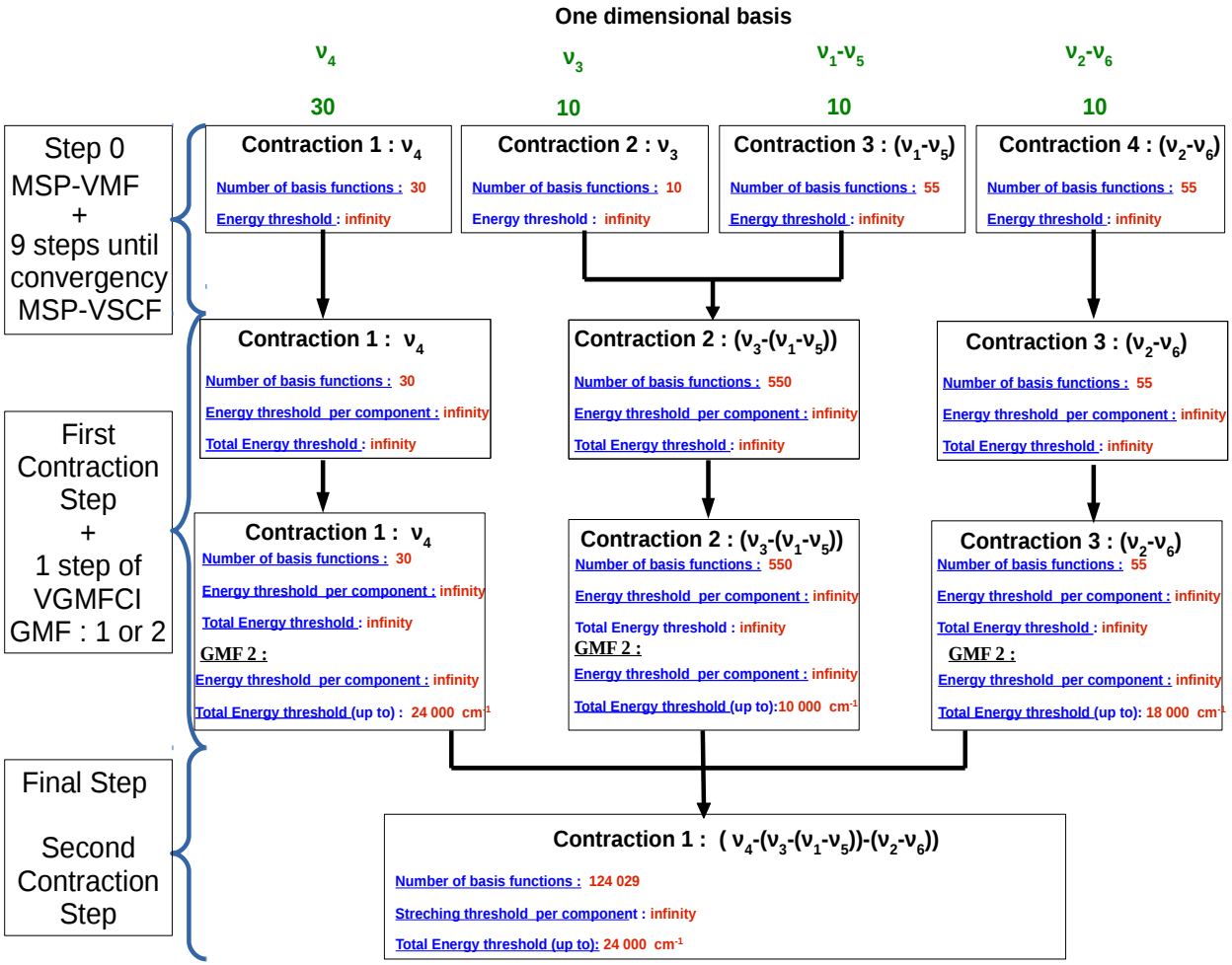

FIG. 2. Schéma de contraction choisi pour la molécule HOOH.

Dans la table II sont reportées les fréquences fondamentales de chaque mode obtenues pour les différentes contractions binaires ainsi que les fréquences obtenues pour le schéma de contraction présenté dans la figure 2.

Dans le première ligne du tableau, sont reportées les ZPE des différentes contractions que l'on comparera à celle du calcul MSP-VSCF. On peut voir que la ZPE ne baisse de manière significative (54.5 cm^{-1}) que pour la contraction (2-4)=(élongation (OO) - pliage (OOH)) tandis que pour les autres contractions, elle baisse d'une valeur allant de 0,12 cm^{-1} jusqu'à 6.6 cm^{-1}. De plus, on observe la même chose pour ce qui concerne les fréquences fondamentales qui sont surtout affectées par la contraction (2-4).

On peut conclure que le mode d'élongation de la liaison (OO) est fortement couplé aux modes de pliage (OOH). Il est donc important de contracter ces modes ensemble. Reste alors les modes de torsion et d'élongation (OH) qui ne seront pas contractés car très peu couplés. Dans ce dernier cas ,il est préférable de les considérer séparément. Ceci allégera le calcul et conservera la qualité de la base MSP-VSCF.

Dans la figure 2 on donne le schéma de contraction optimale et les informations concernant les dimensions des bases pour les différentes étapes jusqu'à la contraction finale.

D. Comparison with other approaches

Pour la suite de l'étude nous utiliserons la configuration de référence de Malyszek. Un calcul pour l'hamiltonien d'ordre trois développé à la référence de Malyszek suivant le schéma de contraction de la figure 2 avec troncature finale à 24000 cm^{-1} et un seuil de troncature sur la base produit des spectateurs de 14000 cm^{-1} servira de calcul de référence pour la suite de ce travail.

mode	ref. SEP	Min global	(2)-(1)
(0,1)	5705.822040	5705.823487	0.001447
(0,4)	11.263072	11.265052	0.001980
(1,1)	255.556462	255.562183	0.005721
(1,4)	371.402667	371.416221	0.013554

		$\{(1-2),(3-4)\}$		$\{(1-3),(2-4)\}$		$\{(1-4),(2-3)\}$		$\{(1,(2-4),3\}$		
Mode	**MSP-VSCF**	(1-2)	(3-4)	(1-3)	(2-4)	(1-4)	(2-3)	(1)	(2-4)	(3)
(0,1)	5770.558274	5770.437182	5768.875634	5770.340211	5716.070834	5763.969691	5770.474770	5770.557735	5716.070834	5770.557754
(0,4)	10.777587	10.827043	-	10.854124	-	11.095368	-	10.789742	-	-
(1,1)	266.672467	266.176208	-	266.288816	-	257.912455	-	266.628030	-	-
(1,4)	382.087091	381.878514	-	381.746824	-	372.787361	-	382.096342	-	-
ν_3	936.366042	935.944771	-	-	866.206830	-	934.987517	-	866.206830	-
ν_6	1276.222508	-	1272.128083	-	1272.624858	1272.496949	-	-	1272.624858	-
ν_2	1450.815225	-	1444.114809	-	1408.889841	1443.680451	-	-	1408.889841	-
ν_1	3604.739283	-	3609.046645	3604.215047	-	-	3605.752041	-	-	3604.739286
ν_4	3610.192123	-	3613.554651	3609.167974	-	-	3610.145204	-	-	3610.190207

TABLE II. Résumé des résultats de calcul en cm^{-1} pour différents schémas de contraction.

(2,1)	570.583715	570.604692	0.020977
(2,4)	777.054603	777.082097	0.027494
ν_3	865.974451	865.975976	0.001525
ν_6	1264.195964	1264.196473	0.000509
ν_2	1395.175366	1395.176062	0.000696
ν_1	3610.827640	3610.828999	0.001359
ν_4	3612.077612	3612.077927	0.000315

TABLE III. Résumé des résultats de calcul en cm^{-1} du schéma de contraction optimale avec troncature à 12000 cm^{-1} pour différentes géométries de référence. L'état (0,1) correspond à l'état fondamental de HOOH. La dernière colonne représente les différences algébriques $E_{Minglobal} - E_{ref.SEP}$.

E. Influence de l'ordre de l'ICCE

Nous allons nous intéresser à présent à l'influence du champ effectif d'ordre deux sur le spectre vibrationnel de HOOH. L'ordre deux permet de prendre en compte le couplage entre l'état fondamental et les états excités des spectateurs. Afin de garder un contrôle sur la taille de la base des spectateurs des seuils de troncature sur l'énergie ont été définis pour chaque spectateur ainsi qu'un seuil sur la somme des énergies des spectateurs.

Nous allons restreindre cette étude à la deuxième itération après la première contraction (voir figure 2) car nous estimons qu'une itération est suffisante pour avoir la convergence du processus MSP-MFCI pour cette contraction.

Nous avons testé différents seuils de troncature sur les fonctions de bases des modes spectateurs pour un même calcul, i.e. mêmes itérations précédentes et même seuils de troncature sur les bases des modes actifs.

Les résultats des différents calculs sont résumés dans les tables IV, V et VI. Dans chaque table, sont reportées les fréquences fondamentales de la contraction que l'on pourra comparer aux fréquences obtenues par une calcul en champ effectif d'ordre un. Pour une contraction donnée, i.e. une table donnée, le seuil de troncature sur les spectateurs est donné en cm^{-1} sur la deuxième ligne.

On peut déduire de ces tables que le champ effectif d'ordre deux a une influence non négligeable, que ca soit sur le fondamental ou sur les états excités. On observe également que la ZPE peut être plus basse que celle de la contraction finale. Ceci est tout à fait normal car avec un champ effectif d'ordre deux la méthode n'est plus variationnelle. On observe que pour la torsion les différences d'énergie entre états excités sont beaucoup plus proches des valeurs convergées. Ceci n'est pas le cas pour les autres contractions, où l'on observe la tendance contraire. Ce dernier résultat s'explique par le fait que les dénominateurs de la série perturbative sont petits (pas de bonne séparation d'énergie entre le fondamental et les niveaux spectateurs correspondant à la torsion) et donc la série converge mal.

Nous constatons que même les seuils les plus bas sont suffisants pour obtenir une convergence au centième de cm^{-1} pour la contraction (OO-OOH) et beaucoup mieux pour les autres contractions.

Pour la suite de l'étude, tenant compte des résultats des tables IV, V et VI et tenant compte du fait que dans un même calcul il est possible de mélanger le champ effectif d'ordre un et deux, i.e. pour certaines contractions, le champ effectif est d'ordre un et

pour les autres il est d'ordre deux, nous avons choisi d'utiliser un champ effectif d'ordre deux pour la torsion et un champ effectif d'ordre un pour les autres modes.

	ordre 1	ordre 2			ICCE
troncature (cm^{-1})	-	14000	20000	24000	24000
(0,1)	5716.061532	5703.845563	5703.844638	5703.844609	5705.794849
(0,4)	10.542326	11.312001	11.312030	11.312032	11.242203
(1,1)	268.224896	255.197460	255.197327	255.197318	255.543418
(1,4)	382.754297	371.522202	371.522184	371.522182	371.353725
(2,1)	589.026024	570.412650	570.412612	570.412608	570.487003
(2,4)	801.717104	777.121932	777.121910	777.121907	776.930930

TABLE IV. Niveaux d'énergie de torsion (cm^{-1}) en champ effectif d'ordre deux en fonction du seuil de troncature de la base produit des spectateurs. Le seuil de 24000 cm^{-1} représente le seuil de troncature sur la base des actifs pour la contraction finale. L'état (0,1) correspond à l'état fondamental de HOOH.

	ordre 1	ordre 2			ICCE
troncature (cm^{-1})	-	8000	10000	14000	24000
ZPE	5716.065998	5667.692921	5667.692615	5667.683225	5705.794849
ν_3	866.195408	854.361847	854.361769	854.359574	865.974776
ν_6	1272.619163	1268.800577	1268.800557	1268.788979	1264.207193
ν_2	1408.885441	1335.736788	1335.736777	1335.719131	1395.147434

TABLE V. Fréquences fondamentales de la contraction (OO - OOH) (cm^{-1}) en champ effectif d'ordre deux en fonction du seuil de troncature de la base produit des spectateurs. Le seuil de 24000 cm^{-1} représente le seuil de troncature sur la base les actifs pour la contraction finale.

	ordre 1	ordre 2			ICCE
troncature (cm^{-1})	-	14000	18000	20000	24000
ZPE	5716.064665	5697.977870	5697.977870	5697.977870	5705.794849
ν_1	3605.246606	3582.685777	3582.685777	3582.685777	3610.689125
ν_4	3610.672233	3604.667245	3604.667245	3604.667245	3611.954087

TABLE VI. Fréquences fondamentales des modes d'élongation OH (cm^{-1}) en champ effectif d'ordre deux en fonction du seuil de troncature de la base produit des spectateurs. Le seuil de 24000 cm^{-1} représente le seuil de troncature sur la base des actifs pour la contraction finale.

Nous allons nous intéresser à présent aux résultats de la contraction finale i.e. l'interaction de configuration vibrationnelle (VCI). Comme on peut le voir dans la table VII, les différences entre les valeurs obtenues avec un champ effectif d'ordre un et celles obtenues avec un champ effectif d'ordre deux pour la torsion sont petites (de l'ordre du dixième de cm^{-1}). De plus, comme on peut le voir dans la figure 3, le ratio de la somme des projection sur la nombre d'état (voir la section ZZZ) pour la VCI après l'ordre deux est toujours supérieur à celui de la VCI après l'ordre un. Ceci montre que les fonctions d'ondes obtenues avec un champ effectif d'ordre deux sont meilleures que celles obtenues avec un champ effectif d'ordre un.

Si l'on compare les valeurs de l'énergie obtenues en champ effectif d'ordre un et deux à celles de référence (voir table VII, on remarque que la configuration d'interaction précédée d'un champ effectif d'ordre deux avec un seuil troncature sur la base produit des actifs de 12000 cm^{-1} est très proche de la référence et meilleure que le calcul précédé d'un champ effectif d'ordre un, ce qui montre que l'influence du champ effectif d'ordre deux est plus importante que l'influence de la dimension de la base qui est quinze fois plus grande dans le calcul de référence.

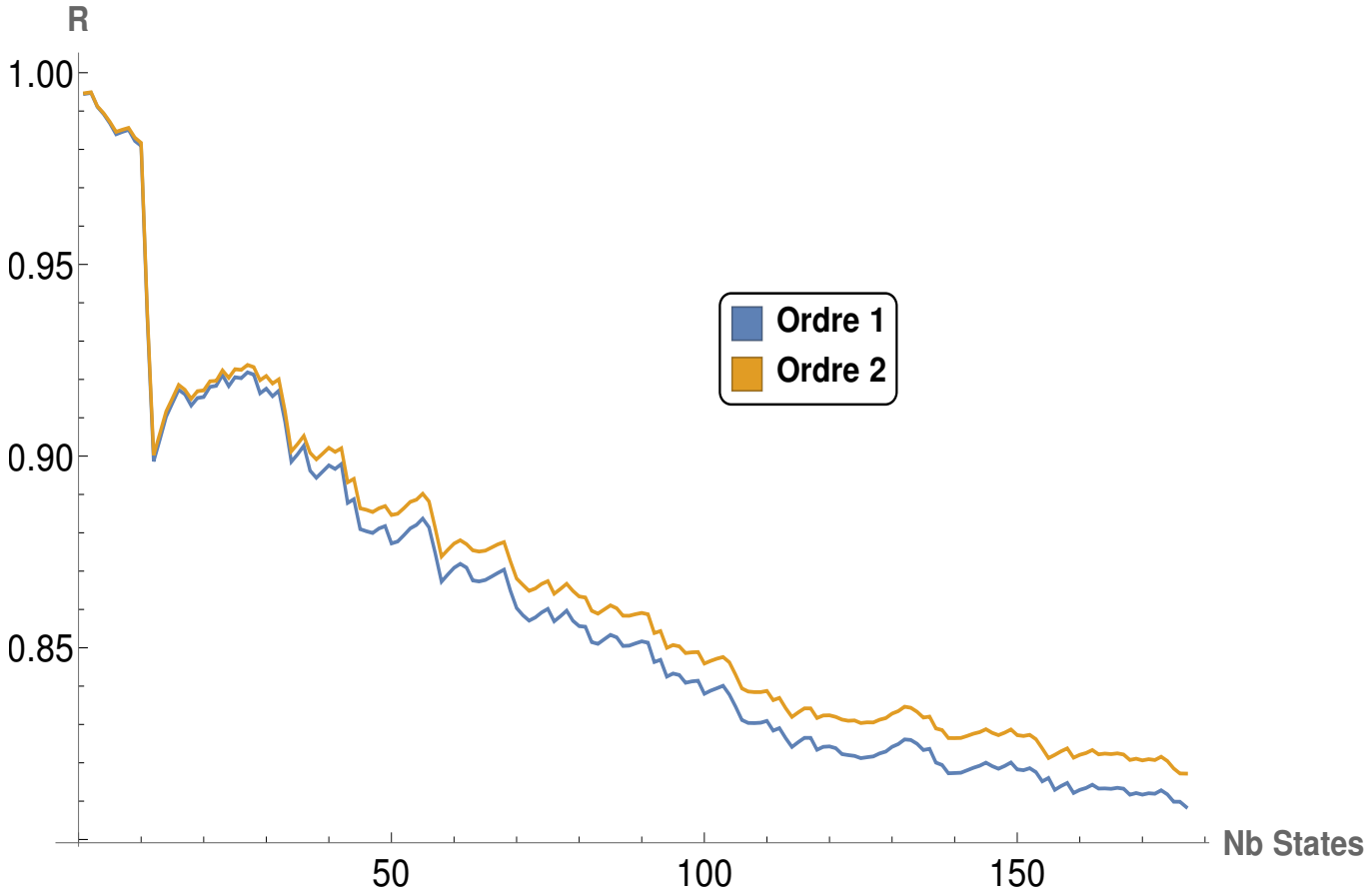

FIG. 3. Évolution du ratio de la somme des projection sur le nombre d'état en fonction du nombre d'état de la configuration vibrationnelle en champ effectif d'ordre un et deux. Le seuil de troncature sur la base produit des spectateurs est de 20000 cm^{-1} et le seuil de troncature sur la base produit des actifs est de 24000 cm^{-1}.

	ICCE ord 1		ICCE ord 2		ICCE reference
Troncature (cm^{-1})	12000		12000		24000
Nb functions	8056		8281		124029
ZPE (cm^{-1})	5705.822040	0.027191	5705.800104	0.005255	5705.794849
	11.263072	0.020869	11.242069	-0.000134	11.242203
	255.556462	0.013044	255.543926	0.000508	255.543418
	371.402667	0.048942	371.354445	0.000720	371.353725

570.583715	0.096712	570.487719	0.000716	570.487003
777.054603	0.123673	776.931839	0.000909	776.930930
865.974451	-0.000325	865.975893	0.001117	865.974776
877.763279	0.019818	877.744213	0.000752	877.743461
1002.096067	0.171792	1001.925715	0.001440	1001.924275
1120.256724	0.014330	1120.244874	0.002480	1120.242394
1227.219451	0.140073	1227.081772	0.002394	1227.079378
1245.607793	0.138526	1245.471876	0.002609	1245.469267

1264.195964	-0.011229	1264.211503	0.004310	1264.207193
1284.635256	0.013220	1284.625973	0.003937	1284.622036
1395.175366	0.027932	1395.157181	0.009747	1395.147434
⋮				
2157.548341	0.687306	2156.883795	0.022760	2156.861035
2172.637162	0.219638	2172.458300	0.040776	2172.417524
2242.704165	0.062879	2242.688225	0.046939	2242.641286
2249.202418	0.078628	2249.169904	0.046114	2249.123790
2277.411464	0.130535	2277.298576	0.017647	2277.280929
⋮				
2907.597101	0.126066	2907.515606	0.044571	2907.471035
2909.981460	0.115238	2909.943416	0.077194	2909.866222
2914.583433	0.118941	2914.569441	0.104949	2914.464492
2918.368706	0.170668	2918.258478	0.060440	2918.198038
⋮				
3597.813695	0.245341	3597.678976	0.110622	3597.568354
3608.096205	0.108494	3608.059420	0.071709	3607.987711
3610.827640	0.138515	3610.818681	0.129556	3610.689125
3612.077612	0.123525	3612.070621	0.116534	3611.954087
3618.982273	0.151362	3618.955908	0.124997	3618.830911
3620.248800	0.142341	3620.223489	0.117030	3620.106459
⋮				
3667.811994	0.504917	3667.412284	0.105207	3667.307077
3677.867902	0.315632	3677.682584	0.130314	3677.552270
3680.492296	0.784734	3680.002916	0.295354	3679.707562
3701.067466	0.756937	3700.512160	0.201631	3700.310529
⋮				

	3978.891546	0.225191	3978.842165	0.175810	3978.666355
	3988.896110	0.430051	3988.758789	0.292730	3988.466059
	3991.091183	0.570245	3990.656874	0.135936	3990.520938
	3999.040176	0.563655	3998.999829	0.523308	3998.476521
	3999.314672	0.431523	3999.009460	0.126311	3998.883149
RMS	–	0.086328	–	0.014141	–

TABLE VII. Spectre $J = 0$ de la molécule HOOH pour une même troncature finale après un champ effectif d'ordre un et deux. La dernière ligne représente la RMS par rapport à l'ICCE de référence.

Ainsi avec une base d'ordre deux sur la torsion, la base produit de dimension réduite (environ 8000) donne un résultat sensiblement équivalent à la référence qui correspond à une VCI de dimension environ 124000. l'outil perturbatif introduit dans cette thèse pour la méthode ICCE est donc avantageux dans le cas d'une séparation d'échelle d'énergie entre deux familles de degrés de liberté.

A titre indicatif, les RMS de l'ICCE ordre 1, l'ICCE ordre 2, l'ICCE de référence par rapport aux valeurs observées sont resp. 1.59559, 1.51824 et 1.47324 . Cet écart par rapport aux valeurs observées peut provenir du manque de précision de la SEP, du choix de la géométrie de référence d'une mauvais paramétrisation de la base initiale, de l'ordre du développement choisi (ordre trois) ou de l'influence de la rotation de la molécule négligée dans ce calcul.

IV. APPLICATION TO NAPHTHALENE VIBRATIONAL SPECTRUM

Naphtalene has the symmetry point group D2h, and we have to find the irreducible representation (irrep) of each normal mode and related harmonic frequencies, not only to reorder the modes in the conventional spectroscopic ordering, but also to take advantage of the symmetry in our calculations. That is to say, the Hamiltonian commuting with all the symmetry operation of the D2h group, it has a block-diagonal diagonal structure, each block corresponding to a different irreps. So, instead of diagonalizing the total Hamiltonian matrix we just have to diagonalize the eight blocks corresponding to the eight irreps. To do that, we made a python program, which find the good symmetry of every frequencies.

As said before, to build the vibrational Hamiltonian, we need a force field derived from electronic calculations. In our case, we used Falvo's data : third and fourth orders constants and harmonic frequencies, to make the anharmonic Hamiltonian. He performed electronic calculations by using the density functional theory (DFT), not explain here, with the basis TZ2P and the functional B97-1, by as implemented in the commercial software Gaussian.

We have written a python program, which transforms Falvo's data in the atomic units, and in a format, either compact or extended, readable by CONVIV. Since the cubic and quartic force constants were not symmetry adapted and were suffering from small numerical errors, we had to purify whose not allowed by symmetry, (in practice, we have retained in a first automatic screening the cubic constants superior than 5.2 10 ?7, and the quartic ones more than 3.8 10 ?8 in absolute values). Then we have cleaned

it manually, searching in the file, the constants in the range of 10 ?7 for the cubic ones and 10 ?8 for the quartic ones, checking if they were allowed by symmetry.

In order to have the spectrum, we also need intensities, so we made a python program which also transforms the first order and second order Falvo's constants of the three components of the dipole moment operator in a format acceptable by CONVIV.

After getting the Hamiltonian and the electric dipole momentum, we performed a VSCF calculation, that is to say, we iterated the partition of all vibrationnal normal modes into singleton until convergence the ZPE of every mode to the same value to machine precision. It took nine iterations to converge the ZPE to about 10 ?7 cm ?1 , and obtain a self-consistent set of reference functions for the normal modes.

At the 10^{th} step we had to start contracting modes together, so, we used a python program to test every possible contraction into a pair of modes. After, we collected the ZPE of all pairs, we sorted them in increasing order to see which contraction pairs were lowering the ZPE the more efficiently. We did it both for the Naphtalene, and its cation form. But, after the thirteenth step, there is not a big gap between the ZPE values of all posible pairs, and the ZPE lowering criterium is not sufficient to determine the best contractions to do. Therefore, we made a python program in order to compare the variation of the frequencies before and after contraction in pair, for all possible pairs, and up to the fifth excited state. So, we first compare the ZPE, and then we study excited states by excited state, the variation of the frequencies.

Note that for each contraction partition selected, we iterated the partition once. Then, the ZPE values of all the contractions were equal to within 10 ?3 cm ?1 . We considered that this convergence was enough and that the calculations within these steps could be legitimately called vibrational self consistent field configuration interaction (VSCFCI). In the end, we did a vibrational configuration interaction (VCI) step, that is to say we contracted all modes (contracted before, or never contracted) together.

In the code CONVIV, we can choose the basis functions we want to use, and many eigenvectors we want to calculate and keep for the next step. As said before, here, we have chosen for the initial step a basis of harmonic oscillator eigenfunctions (there are other choices available in the CONVIV code, but for our calculations, harmonic eigenfunctions were suitable). In order to avoid missing levels "holes" under a certain energy in the spectrum, we took fifteen basis functions for the frequencies more than 1000 cm^{-1}, twenty basis functions for frequencies which are between 500 cm^{-1} and 1000

cm^{-1}, and we took thirty basis functions for frequencies less than 500 cm^{-1}.

For every new contractions we made, we had to do truncations, in order to control the growth of the size of the product basis as the number of contracted modes increases. We made truncations on the sum of the eigenvalues. Moreover, we have to specify the number of eigenvectors we wanted to save at the end of each contraction, because saving all the vectors, if the basis set is large, takes too much RAM memory, and it is useless since these eigenvectors will not be used in the following step. In the next sections, we will particularly discuss the C-H stretches, because researchers think that they are responsible for the emission band observed at 3.3 μm ($\sim$3000 cm^{-1})[132].

A. The force field precision

In this part, we will compare the results obtained using the Falvo's force field[129], and the Mackie one[130], up to the thirteenth step (we made the same contractions up to this step, see below to details of the contraction), in order to discuss the force field precision. Since Falvo and Mackie did not use the same functional nor basis to make their calculations. This comparison will permit us to give us an order of magnitude of the precision we can expect. More precisely, Mackie used the functional B3LYP and the basis N07D, whereas Falvo used the functional B97-1 and the basis TZ2P. As we can see in the TABLE. II, the root mean square (RMS) error is smaller as we contract modes. In fact, at the VSCF step, the RMS is 8.9 cm^{-1}, and after 2 VMFCI steps, the RMS is 7.4 cm^{-1}. On average, we can not expect a precision better than 7.4 cm^{-1}. However, the precision may depend on the frequency and/or the . Therefore, we have calculated the mean deviation between results obtained for stretches only and for other modes below and above 1000 cm^{-1} separetely to have a more detail idea of the maximal convergence we can expect. Therefore we not try to achive in our calculations a convergence better than 6 cm^{-1} for CH stretches, 3 cm^{-1} for ones over 1000 cm^{-1} and 1 cm^{-1} for modes less 1000 cm^{-1}.

We used the Falvo's force field for our study because we wanted to compare the cation and the neutral forms, and only Falvo's made calculations for the ionised naphtalene.

B. Sensitivity to force field truncatures

Cané et al. used exactly the same electronic method than Falvo that is B97-1/TZ2P DFT level of theory. However, Cané et al. retained only the largest force field constants, so Hamiltonian has about only 4000 terms whereas Falvo has about 10500 terms after cleaning which is about the same as Mackie Hamiltonian. So, performing exactly the same calculation for the Falvo and the Cané Hamiltonian will permit us to assess the sensitivity to the truncatures of the force field. As we can see inspecting the last colomn of TABLE. II, they can be large differences between the two calculations. In particular, the differences between ν_1 is 12.6 cm^{-1} and the RMS error is 4.7 cm^{-1}. The very good agreement between Cané's results and experiment is probably due to error compensations.

C. Naphtalene's neutral form : comparison between steps and with experiment

In this part, we compare between themselves ZPE and frequencies at different stages of the calculations. We also compare our final results to experiment.

For the neutral form, we did :

VSCF/VSCFCI11({1,17,29,37};36000.0,{2,30};36000)/VSCFCI13({1,2,17,18,29,30,37,38};36000.0)/VS
11,15,17,18,29,30,37,38,46};16800.0,{5,8},{26,27})/VSCFCI17({1,2,10,11,14,15,17,18,25,26,27,29,30,37,38,
{3,5,8,19,32,33,39};15160.0,{4,6,9,40,48},18800.0,{7,13,16,28,31,35};10710)/VCI(4200;1650)

In the previous notation, we separated the important step by a "/", and we put the contractions made in "{}", and separated the component number and the associated constraint by a ";". As said before, the constraint is on the sum of the eigenenergies of the contracted components, except for the VCI step, where we put two constraints : the first on the sum of all the eigenenergies of all the components, and the second on the sum of the eigenenergies of all the components, except the first one, which contains the CH stretches.

Let us give more details about what we did exactly. First, we performed VSCF calculation which took nine steps to converge, then, we used a python program to test every possible contraction into a pair of modes, as explained before. Next, we did a VSCFCI calculation (called VSCFCI11), where we have contracted separately the modes 1, 17, 29, 37 with 36000 as constraint, and the modes 2, 30 with the same constraint, immediately followed by the VSCFCI13 calculation, where all CH stretches have been

contracted together. For these two partitions, we used the ZPE criteria to determine the contractions we had to do and we can see in TABLE III that the ZPE decreased by 71.4 cm^{-1}. Moreover, the CH stretches frequencies decrease on average by 112.5 cm^{-1} between the VSCF step and the thirteen one (VSCFCI13), with a maximum lowering of 118.7 cm^{-1}.

After these steps, we used another criteria : the variation of the frequencies (up to the fifth excited state) before and after contraction pair, by using a python program we have written. We did a VSCFCI step (called VSCFCI15) where we contracted the modes 11, 15 and 46 with the others already contracted (which form now a new partition of contractions, as explained in the theory part). We put 16800 cm^{-1} as a constraint threshold of the sum of the energy, and we also made two others contractions, the modes 5, 8 and the modes 26, 27, both without constraint. We can see in TABLE III that CH stretches generally re-increased as expected, such as ν_{29} which increased by 6.8 cm^{-1}. Whereas the other modes we contracted, such as ν_{11}, decreased a lot (22.6 cm^{-1}).

Then, we did a last VSCFCI calculation (VSCFCI17) where we contracted modes 10, 14, 25, {26, 27} (which are already contracted together), and 45. We put 9136 cm^{-1} as constraint threshold , because we wanted to have at least the first three excited states of the CH stretches. We also contracted separately the modes 3, {5, 8} (which were already contracted together), 19, 32, 33, 39, with 15160 as constraint, the modes 4, 6, 9, 40, 48 with 18800 cm^{-1} as threshold, and the modes 7, 13, 16, 28, 31, 35 with 10710 cm^{-1} as threshold. We can see in the TABLE III that the CH stretches continue to re-increase, for example, ν_{30} which re-increase from 2955.0 cm^{-1} to 2970.8 cm^{-1} (15.8 cm^{-1}). As before, the other modes newly contracted generally decreased, such as the mode ν_{10}, which decreased from 1020.3 cm^{-1} to 976.9 cm^{-1} (43.4 cm^{-1}).

To finish, we did a VCI step to contract all modes, with 4200 cm^{-1} as truncation threshold on the sum of all component energies, and 1650 as truncation threshold on the sum of all components expect the first (which contains CH stretches).

Even thought we did not use the ZPE lowering criterion after the VSCFCI13 step, we can see in TABLE III that the ZPE continue to decrease. Actually, it decreased from 32029.8 cm^{-1} (VSCF step) to 31866.0 cm^{-1} (VCI step).

We can see, when we compared experiment to our preliminary results in TABLE. III that CH stretches are overestimated compared to experiment, the deviation is, in average (for the CH stretches only) about 61.6 cm^{-1}. We are aiming at a convergence to about 6 cm^{-1}.

D. Comparison between cation and neutral forms of naphtalene

In this last subsection, we will compare the results obtained for the cation and the neutral form of the naphtalene, comparing their spectra.

For the ionised form, we did :

VSCF/VSCFCI11({1,17,29,37};36000,{2,30,38};36000)/VSCFCI13({1,2,17,18,29,30,37,38};36000)/VSC
10,11,15,17,18,29,30,37,38,46}16800;,{3,7,12,23,32};22300,{4,5,8,16,39};21540,{6,13,34,36,48};11521,{9,19,
21590,{14,45,47},{22,42},{25,26,27,28};20940)/VCI(4500;1600)

For the cation, following exactly the same process, we found that we had to contract the CH stretches first but not in the same order. Moreover, for the neutral form, we did eighteen steps, and for the ionised one we only did sixteen steps.

We can compare the cation FIG 4 and neutral FIG 5 form using their spectra. In fact, we can see nearly the same peaks, but not with the same intensity (the most intense peak is set to the maximum and the intensity of the others are scaled accordingly, for the neutral form, the peak which is around 3000 cm $^{-1}$ is less intense than for the ionised form, where it is the most intense), and with a shift. For example, we observe a peak at 1776.5 cm $^{-1}$ for the neutral naphtalene, and one at 1784.7 cm $^{-1}$ for the ionised one.

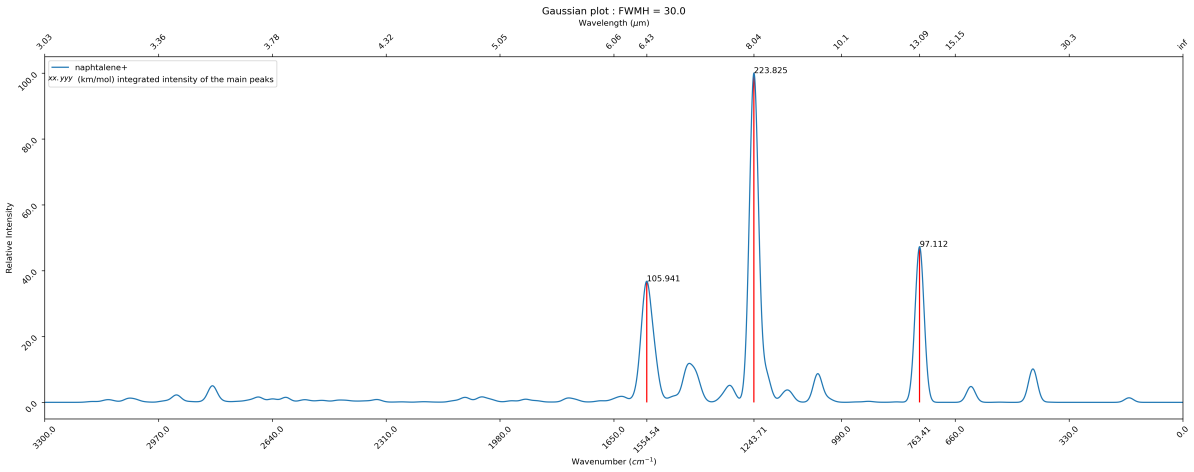

FIG. 4. Theoretical spectra obtained for the ionised form of naphtalene.

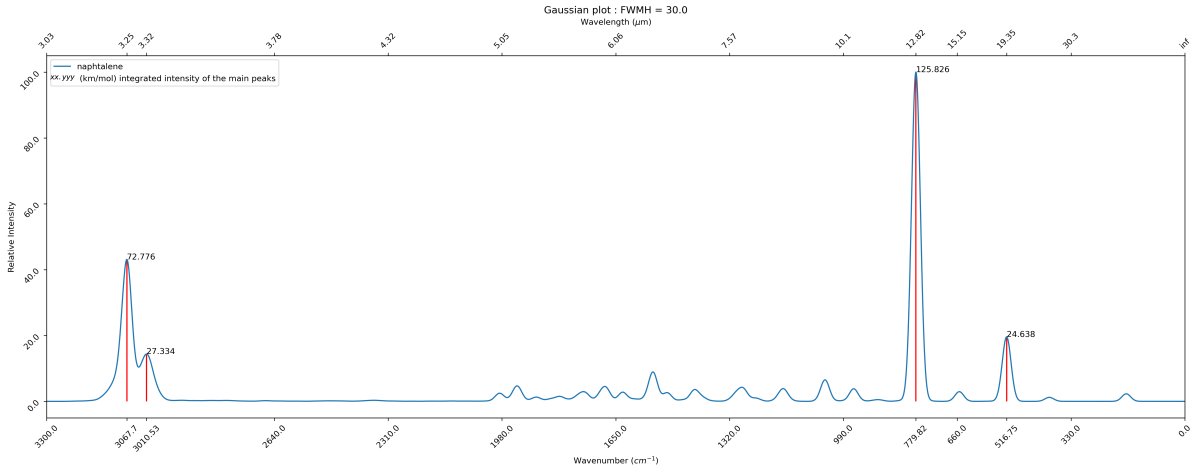

FIG. 5. Theoretical spectra obtained for the neutral form of naphtalene.

V. CONCLUSION

When strong resonances occur in a quantum system, perturbative approximations are usually inappropriate. Perturbative series are known to converge poorly even in some simple cases, where in addition, no resummation technique is able to cover efficiently the full range of the parameter space[117,118].

When small energy differences relative to total energy occur, that is to say, typically, when two well-separated energy scales are present in a physical problem, the CI method may encounter numerical instabilities, due to a possibly ill-conditionned CI matrix. However, in such a situation, one is usually able to find a small parameter amenable to a rapidly converging pertubative expansion. Perturbative approaches are also better suited when the Hamiltonian is not bounded from below, as is often the case in relativistic systems, but also in vibrational Hamiltonians, whenever the potential is fitted with polynomials[18]. Finally, of course, when a large number of eigenstates is sought after, the computational cost of a perturbation method can be more advantageous than that of CI, the latter scaling at best as the CI matrix dimension to the power 3.

The increased flexibility of the GMFCI method with respect to MFCI allows one to take the best of two worlds, the perturbative and the variational ones. Our implementation of what we had called the "generalized perturbation method to non-commutative rings", was in fact a particular case of GMFCI calculation with a GMF of order 4, as shown in section 3. The numerical results presented here, with an improved DMS, confirm the reliability of the predictions made with our approach.

In practice, beside the rotation-vibration DOF partitioning explored in this article, we expect GMFCI to perform better than the simple MFCI approach for floppy systems,

with large amplitude motion, or more generally, when slow and rapid motions are coupled in the same system. Work is in progress on hydrogen peroxyde, where, beside rotational DOF, a torsional DOF is coupled to the bending and stretching internal motions.

ACKNOWLEDGEMENTS

This work was supported by the grant CARMA ANR-12-BS01-0017. The author acknowledge the SIGAMM Mesocentre for hosting the CONVIV code project and the JAD laboratory computer facilities (J.-M. Lacroix and J. Maurin). This work was granted access to the HPC and vizualization resources of the "Centre de Calcul Interactif" hosted by University Nice Sophia Antipolis. The authors are grateful to Prof. J. Koput for providing the HOOH PES. Prof. Bernie Shizgal is acknowledged for contributing to the chebychev quadrature integration code. This work has been supported by the French government, through the UCAJEDI Investments in the Future project managed by the National Research Agency (ANR) with the reference number ANR-15-IDEX-01.

REFERENCES

[1]P. W. Higgs, J. Chem. Phys **21**, 1131 (1953)

[2]P. W. Higgs, J. Chem. Phys **23**, 1448 (1955)

[3]P. W. Higgs, J. Chem. Phys **23**, 1450 (1955)

[4]J. M. Bowman, K. Christoffel, F. Tobin,J. Phys. Chem. **83**, 905-912 (1979)

[5]B. Maessen, and M. Wolfsberg,J. Phys. Chem. **89**, 3876 (1985)

[6]C. L. Chen, B. Maessen, and M. Wolfsberg,J. Chem. Phys **83**, 1795-1807 (1985)

[7]J. Tennyson, B. Sutcliffe Mol. Phys. **58**, 1067 (1986)

[8]Z. Bačić and J. C. Light, J. Chem. Phys **85**, 4594 (1986)

[9]Richard A. Friesner, Joseph A. Bentley, Michel Menou and Claude Leforestier, J. Chem. Phys **99**, 324 (1993)

[10]Matthew J. Bramley and Tucker Carrington Jr, J. Chem. Phys **101**, 8494 (1994)

[11]X.-G. Wang, T. Carrington Jr., J. Chem. Phys **117**, 6923 (2002)

[12]X.-G. Wang, T. Carrington Jr., Int. J. Quantum Chem. **99**, 556 (2003)

[13]X.-G. Wang, T. Carrington Jr., J. Chem. Phys **119**, 101 (2003)

[14]X.-G. Wang, T. Carrington Jr., J. Chem. Phys **121**, 2937 (2004)

[15]Hua-Gen Yu, Chem. Phys. Lett. **365**, 189-196 (2002)

[16]P. Cassam-Chenaï and J. Liévin, Int. J. Quantum Chem. **93**, 245-264 (2003)

[17]P. Cassam-Chenaï, J. Liévin, Journal of Computational Chemistry **27**, 627-640 (2006)

[18]P. Cassam-Chenaï, A. Ilmane, J. Math. Chem. **50**, 652 (2012)

[19]G. D. Carney, L. L. Sprandel and C. W. Kern in Advances in Chemical Physics, Vol. 37, I. Prigogine and S.A. Rice, Eds., (Wiley, New York, 1978), pp. 305-379.

[20]J. M. Bowman, J. Chem. Phys **68**, 608-610 (1978)

[21]J. M. Bowman, B. Gazdy, J. Chem. Phys **94**, 454-460 (1991)

[22]P. Cassam-Chenaï, J. Quant. Spectrosc. Radiat. Transfer **82**, 251-277 (2003)

[23]D. Bégué, C. Pouchan, N. Gohaud, P. Cassam-Chenaï, J. Liévin, J. Chem. Phys **127**, 164115-164124 (2007)

[24]P. Cassam-Chenaï, Yohann Scribano, Jacques Liévin, Chem. Phys. Lett. **466**, 16 (2008)

[25]P. Cassam-Chenaï, J. Math. Chem. **49**, 821 (2011)

[26]P. Cassam-Chenaï, Y. Bouret, M. Rey, S. A. Tashkun, A. V. Nikitin, VL. G. Tyuterev, Int. J. Quantum Chem. **2201-2220**, 112 (2012)

[27]P. S. Thomas, T. Carrington Jr., J. Chem. Phys **146**, 204110 (2017)

[28]M. Odunlami, V. Le Bris, D. Bégué, I. Baraille, O. Coulaud, J. Chem. Phys **146**, 214108 (2017)

[29]V. Le Bris, M. Odunlami, D. Bégué, I. Baraille, O. Coulaud, Phys. Chem. Chem. Phys. **22**, 7021-7030 (2020)

[30]P. S. Thomas, T. Carrington Jr., J. Agarwal, H. F. Schaefer, J. Chem. Phys **149**, 064108 (2018)

[31]E. Lesko, M. Ardiansyah, K. R. Brorsen, J. Chem. Phys **151**, 164103 (2019)

[32]J. K. G. Watson, Mol. Phys. **103**, 3283 (2005)

[33]J. H. Van Vleck, Phys. Rev. **33**, 467 (1929)

[34]E. C. Kemble, "Fundamentals of Quantum Mechanics" (Dover, New York, 1937), p. 395

[35]J. des Cloizeaux, nucl. phys. **20**, 321 (1960)

[36]H. Primas, Rev. Mod. Phys. **35**, 710 (1963)

[37]L. N. Buleavski, Zh. Eksp. Teor. Fiz. **51**, 230 (1966) [English translation in Sov. Phys. -JETP **24**, P. 154 (1967)].

[38]C. Soliverez, J. Phys. C: Solid State Phys. **2**, 2161 (1969)

[39]D. Klein, J. Chem. Phys **61**, 786 (1974)

[40]Yu. S. Makushkin, Vl. G. Tyuterev, *Perturbation Methods and Effective Hamiltonians in Molecular Spectroscopy*, Nauka, Novosibirsk, (1984) *[in Russian]*.

[41]L. E. Fried, G. S. Ezra, J. Chem. Phys **86**, 6270 (1987)

[42]E. L. Sibert III, J. Chem. Phys **88**, 4378 (1988)

[43]D. Sugny and M. Joyeux, J. Chem. Phys **112**, 31 (2000)

[44]S. V. Krasnoshchekov and N. F. Stepanov, J. Chem. Phys **139**, 184101 (2013)

[45]F. Jørgensen, T. Pedersen, Mol. Phys. **27**, 33 (1974)

[46]I. Shavitt, L. T. Redmon, J. Chem. Phys **73**, 5711 (1980)

[47]S. Kvaal, Phys. Rev. **C78**, 044330 (2008)

[48]F. Jørgensen, Int. J. Quantum Chem. **115**, 1691 (2015) and therein from the same author.

[49]H. Araki, Publ. Res. Inst. Math. Sci. Kyoto Univ. **6**, 385 (1970-71)

[50]P. Cassam-Chenaï, G.S. Chandler, Int. J. Quantum Chem. **46**, 593-607 (1993)

[51]W. H. Shaffer, H. H. Nielsen and L. H. Thomas Phys. Rev. **56**, 895 (1939)

[52]V. N. Bryukhanov and Yu. S. Makushkin, Opt. Spectrosc. **36**, 469-474 (1974)

[53]Yu. S. Makushkin, Opt. Spectrosc. **37**, 662-667 (1974)

[54]O. K. Voitsekhovskaya and Yu. S. Makushkin, Opt. Spectrosc. **39**, 32-37 (1975)

[55]Vl. G. Tyuterev and V. I. Perevalov, Chem. Phys. Lett. **74**, 494 (1980)

[56]Vl. G. Tyuterev, S. Tashkun, M. Rey, R. Kochanov, A. Nikitin, and T. Delahaye, J. Phys. Chem. **A117**, 13779 (2013)

[57]P. B. Changala and J. H. Baraban, J. Chem. Phys **145**, 174106 (2016)

[58]P.-O. Löwdin, J. Chem. Phys **19**, 1396 (1951)

[59]P. Cassam-Chenaï and J. Liévin, J. Chem. Phys **136**, 174309 (2012) and supplementary material.

[60]P. Cassam-Chenaï and J. Liévin, J. Mol. Spectrosc. **291**, 77-84 (2013) And supplementary material.

[61]P. Cassam-Chenaï, G. Rousseau, A. Ilmane, Y. Bouret, M. Rey, J. Chem. Phys **143**, 034107 (2015)

[62]P. Cassam-Chenaï,B. Suo, W. Liu, Phys. Rev. **A**, 92 (012502)2015

[63]N. J. Wright, R. B. Gerber, J. Chem. Phys **114**, 8763 (2001)

[64]A. V. Sergeev, D. Z. Goodson, Mol. Phys. **93**, 477 (1998)

[65]W. Mizukami, D. P. Tew, J. Chem. Phys **139**, 194108 (2013)

[66]M. L. Senent, R. Dominguez-Gómez, Chem. Phys. Lett. **351**, 251 (2002)

[67]A. Samsonyuk, Ch. Scheurer J. Comp. Chem. **34**, 27-37 (2013)

[68]J. C. Light and Z. Bačić, J. Chem. Phys **87**, 4008 (1987)

[69]J. M. Bowman, Chem. Phys. Lett. **217**, 36 (1994)

[70]S. Carter and J. M. Bowman, J. Chem. Phys **108**, 4397 (1998) and therein.

[71]D. Lauvergnat, A. Nauts, Y. Justum and X. Chapuisat, J. Chem. Phys **114**, 6592 (2001)

[72]D. Lauvergnat, A. Nauts, Chem. Phys. **305**, 105-113 (2004)

[73]A. Willetts, Ph. D thesis, University of Cambridge, UK, 1990.

[74]V. Barone, J. Chem. Phys **122**, 14108 (2005)

[75]V. Barone, J. Bloino, C. A. Guido, F. Lipparini, Chem. Phys. Lett. **496**, 157-161 (2010)

[76]M. Piccardo, J. Bloino, V. Barone, Int. J. Quantum Chem. **115**, 948-982 (2015)

[77]C. Fábri, T. Furtenbacher and A. G. Császár, Mol. Phys. **112**, 2462 (2014)

[78]E. Mátyus, G. Czakó, B. T. Sutcliffe, A. G. Császár, J. Chem. Phys **127**, 084102 (2007)

[79]A.I. Pavlyuchko , S.N. Yurchenko, Jonathan Tennyson, Mol. Phys. **113**, 1559 (2015)

[80]S. Brodersen and J.-E. Lolck, J. Mol. Spectrosc. **126**, 405-426 (1987)

[81]C. Pouchan and K. Zaki, J. Chem. Phys **107**, 342 (1997)

[82]I. Baraille, C. Larrieu, A. Dargelos, M. Chaillet, Chem. Phys. **273**, 91 (2001)

[83]Y. Scribano, D. M. Benoit, Chem. Phys. Lett. **458**, 384 (2008)

[84]Michael Neff and Guntram Rauhut, J. Chem. Phys **131**, 124129 (2009)

[85]B. Huron, J.-P. Malrieu, P. Rancurel, J. Chem. Phys **58**, 5745 (1973)

[86]M. Rey, A. V. Nikitin and Vl. G. Tyuterev, Phys. Chem. Chem. Phys. **15**, 10049 (2013)

[87]M. Rey, A. V. Nikitin and Vl. G. Tyuterev, J. Chem. Phys **141**, 044316 (2014)

[88]W. Ritz, Journal für die Reine und Angewandte Mathematik **135**, 1-61 (1909)

[89]https://forge.oca.eu/trac/conviv

[90]M. J. Bramley and T. Carrington Jr, J. Chem. Phys **99**, 8519 (1993)

[91]R. Chen, G. Ma, and H. Guo, Chem. Phys. Lett. **320**, 567 (2000)

[92]R. Chen, G. Ma, and H. Guo, J. Chem. Phys **114**, 4763 (2001)

[93]V. A. Benderskii, E. V. Vetoshkin, I. S. Irgibaeva, H.-P. Trommsdorff Russian Chem. Bull., Int. ed. **50**, 366 (2001)

[94]S. Carter, N. C. Handy, J. Chem. Phys **113**, 987 (2000)

[95]M. Mladenović, Spectr. Chimica Acta **A58**, 809 (2002)

[96]Hee-Seung Lee and J. C. Light, J. Chem. Phys **120**, 4626 (2004)

[97]S. Carter and N. C. Handy, Spectr. Chimica Acta **A60**, 2107 (2004)

[98]S. Carter, N. Handy and J. M. Bowman, Mol. Phys. **107**, 727 (2009)

[99]S. Carter, A. R. Sharma and J. M. Bowman, J. Chem. Phys **135**, 014308 (2011)

[100]M. L. Senent, S. Fernández-Herrera b , Y. G. Smeyers, Spectrochimica Acta **A56**, 1457 (2000)

[101]L. B. Harding, J. Phys. Chem. **93**, 8004 (1989)

[102]A. Ilmane, ph.D thesis, Université Nice Sophia Antipolis, (2015).

[103]D. Lauvergnat, A. Nauts, J. Chem. Phys **116**, 8560 (2002)

[104]William H. Miller, Nicholas C. Handy, and John E. Adams,J. Chem. Phys **72**, 99 (1980)

[105]T. Carrington Jr., W. H. Miller,J. Chem. Phys **81**, 3942 (1984)

[106]D. P. Tew, N. C. Handy, and S. Carter, J. Chem. Phys **125**, 084313 (2006)

[107]G. Simons, R. G. Parr, and J. M. Finlan,J. Chem. Phys **59**, 3229 (1973)

[108]P. Malyszek, J. Koput, J. Comp. Chem. **34**, 337 (2013)

[109]D. Strobusch, Ch. Scheurer J. Chem. Phys **135**, 124102 (2011)

[110]D. Strobusch, Ch. Scheurer J. Chem. Phys **135**, 144101 (2011)

[111]D. Strobusch, M. Nest, Ch. Scheurer J. Comp. Chem. **34**, 1210 (2013)

[112]X. G. Wang et T. Carrington,Mol. Phys. **110**, 825 (2012)

[113]R. Dawes and T. Carrington, J. Chem. Phys **122**, 134101 (2005)

[114]A. Kratzer, Z. Physik 3,(1920) 289

[115]W. H. Shaffer, J. Mol. Spectrosc. **1**, 69 (1957)

[116]See document Number ...

[117]G. A. Arteca, F. M. Fernàndez, E. A. Castro, "Large Order Perturbation Theory and Summation Methods in Quantum Mechanics", (Springer-Verlag, Berlin), Lecture Notes in Chemistry **53**, (1990)

[118]E. J. Weniger, Annals of Physics **246**, 133-165 (1996)

[119]T. J. Lukka, J. Chem. Phys **102**, 3945 (1995)

[120]M. J. Bramley and N. C. Handy, J. Chem. Phys **98**, 1378-1397 (1993)

[121]Julien Bloino, J. Phys. Chem. **A119**, p.5269 (2015)

[122]Henrik G.Kjaergaard and Bryan R. Henry, J. Phys. Chem. **99**, p.899 (1995)

[123]J. M. Flaud, C. Camy-Peyret, J. W. C. Johns, B. Carli, J. Chem. Phys **91**, 1504 (1989)

[124]C. Camy-Peyret, J. M. Flaud, J. W. C. Johns, M. Noël, J. Mol. Spectrosc. **155**, 84 (1992)

[125]A. Perrin, A. Valentin, J. M. Flaud, C. Camy-Peyret, L. Schriver, A. Schriver, Ph. Arcas, J. Mol. Spectrosc. **171**, 358 (1995)

[126]W. B. Olson, R. H. Hunt, B. W. Young, A. G. Maki, J. W. Brault, J. Mol. Spectrosc. **127**, 12 (1988)

[127]W. B. Cook, R. H. Hunt, W. N. Shelton, F. A. Flaherty, J. Mol. Spectrosc. **171**, 91 (1995)

[128]Wolfram Research Inc., Mathematica, Version 12.0, (Champaign, IL, 2019)

[129]C. Falvo, F. Calvo, P. Parneix, J. Chem. Phys **137**, 064303 (2012) and Private communication

[130]C. J. Mackie, T. Chen, A. Candian, T. J. Lee, A. G. G. M. Tielens J. Chem. Phys **149**, 134302 (2018)

[131]M.C. McCarthy, B.A. McGuire, J. Phys. Chem. , ()

[132]A. Li, nature astronomy **4**, 339 (220)

APPENDIX A: 1D-SECTIONS OF THE PES

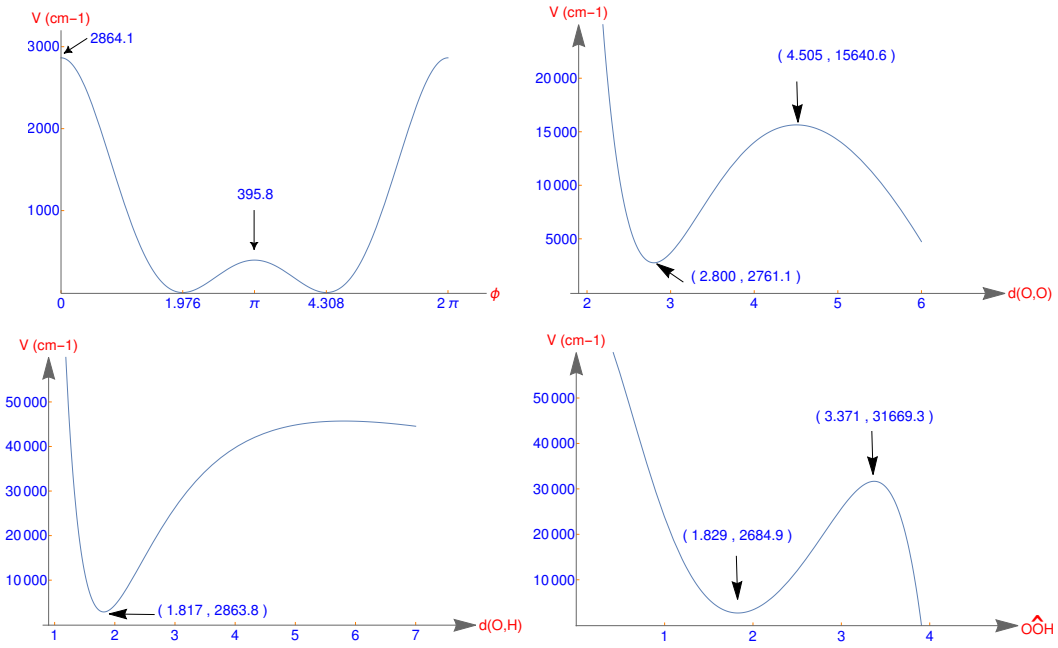

FIG. 6. 1D-Sections of the Malyszek and Koput PES[108].

APPENDIX B: CONVERGENCE EN FONCTION DE L'ORDRE DU DÉVELOPPEMENT

Nous nous sommes proposés dans cette partie d'étudier la convergence des valeurs propres par rapport à l'ordre du développement en les deux angles de liaison OOH et en fonction des termes de l'opérateur cinétique inclus dans l'hamiltonien. Pour un ordre de développement donné nous avons réalisé trois calculs différents. Dans le premier calcul, on ne tient compte que de la matrice $\mathbf{f}_2$, dans le second, on ajoute le vecteur $\mathbf{f}_1$, et dans le troisième, on ajoute le terme extra potentiel (voir la sous-section YYY du chapitre Mathematica). Ces calculs permettront de mesurer l'influence de chacun des termes.

Les figures 7 et 8 montrent l'évolution de la ZPE et de fréquences choisies en fonction de l'ordre du développement en θ_1 et θ_2 de l'opérateur cinétique. La première chose qui apparaît est que le terme dominant en ce qui concerne les différences d'énergie est f_2 suivi par f_1, le terme extra potentiel se placant en dernier : il ne produit essentiellement qu'un déplacement global des valeurs propres. On observe une convergence satisfaisante des fréquences à partir de l'ordre deux. Une convergence quasi-totale est obtenue à partir de l'ordre 4. Ces résultats sont en accord avec ceux de Strobusch et al.[109–111], de même que sur la convergence en fonction de l'ordre du développement.

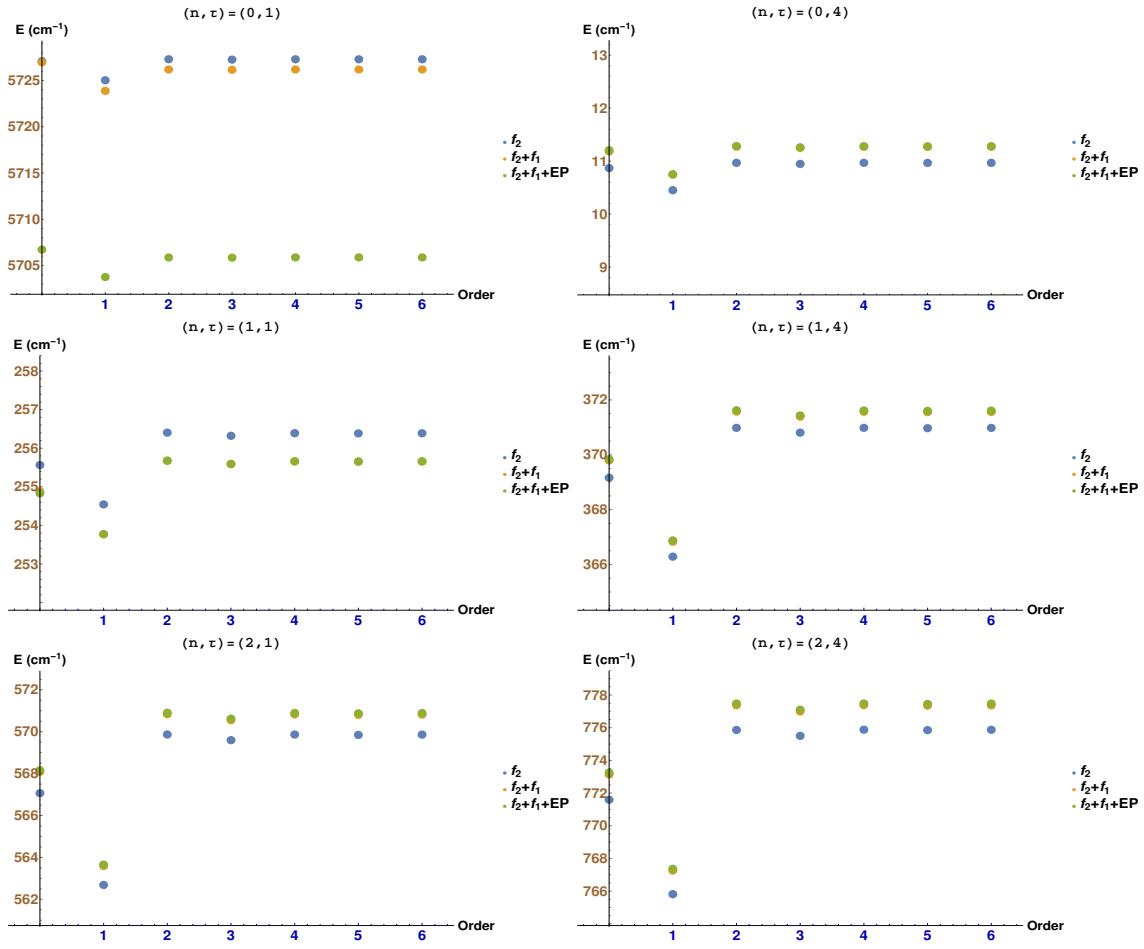

FIG. 7. Évolution de la valeur de l'énergie de torsion en fonction de l'ordre de développement des différents termes de l'opérateur d'énergie cinétique.

.

Nous avons choisi de nous limiter à l'ordre trois dans la suite du travail. Une autre indication que cet ordre est suffisant est donnée dans la table VIII. Le calcul ICCE (24000) de référence qui sera détaillé dans la section XXX montre que les plus grandes différences par rapport aux fréquences de l'hamiltonien original calculées par Malyszek et Koput[108] sont inférieures au cm^{-1}.

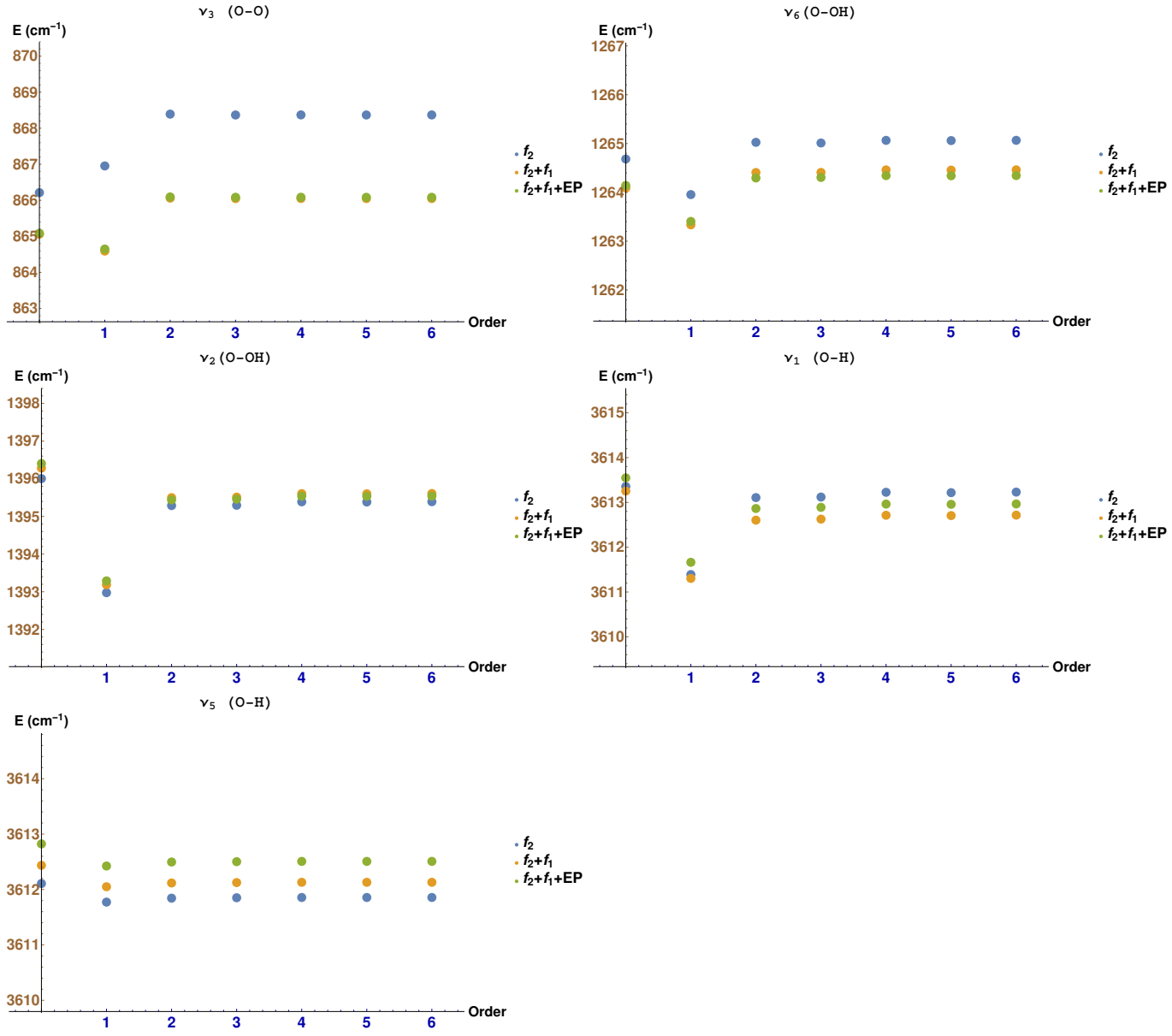

FIG. 8. Évolution de la valeur de l'énergie des mouvements de petites amplitudes en fonction de l'ordre de développement des différents termes de l'opérateur d'énergie cinétique.

ν_1	ν_2	ν_3	ν_4	ν_5	ν_6	ICCE	diff	Malyszek	obs.
0	0	0	1	0	0	255.5	0.1	255.4	254.6
0	0	0	2	0	0	570.5	0.1	570.4	569.7
0	0	1	0	0	0	866.	0.	866.	865.9
0	0	0	3	0	0	1001.9	0.	1001.9	1000.9

A_g

0	0	1	1	0	0	1120.2	0.	1120.2	1117.5
0	1	0	0	0	0	1395.1	0.2	1394.9	1395.9
0	1	0	1	0	0	1683.7	0.1	1683.6	1681.1
0	0	0	0	0	2	2505.1	-0.6	2505.7	2506.3
0	2	0	0	0	0	2766.7	0.4	2766.3	2766.
1	0	0	0	0	0	3610.7	0.1	3610.6	3609.8

A_u	0 0 0 0 0 0	11.2	-0.1	11.3	11.4
	0 0 0 1 0 0	371.4	0.1	371.3	370.9
	0 0 0 2 0 0	776.9	0.	776.9	776.1
	0 0 1 0 0 0	877.7	-0.1	877.8	877.9
	0 0 1 1 0 0	1227.1	-0.1	1227.2	1227.4
	0 1 0 0 0 0	1401.3	0.2	1401.1	1398.3
	0 1 0 1 0 0	1772.9	-0.3	1773.2	1769.8
	0 0 0 0 0 2	2538.2	-0.8	2539.	2539.3
	0 2 0 0 0 0	2770.	0.2	2769.8	2769.5
	1 0 0 0 0 0	3618.8	0.	3618.8	3618.
B_u	0 0 0 0 0 1	1264.2	-0.3	1264.5	1264.6
	0 0 0 1 0 1	1504.9	-0.3	1505.2	1504.9
	0 0 0 2 0 1	1853.6	-0.7	1854.3	1853.6
	0 1 0 0 0 1	2649.2	-0.2	2649.4	2649.
	0 1 0 1 0 1	2914.5	-0.4	2914.9	2913.7
	0 0 0 0 1 0	3612.	0.2	3611.8	3610.7
	0 0 0 1 1 0	3876.9	0.2	3876.7	3875.8
B_g	0 0 0 0 0 1	1284.6	-0.4	1285.	1285.1
	0 0 0 1 0 1	1648.1	-0.6	1648.7	1648.4
	0 0 0 2 0 1	2072.1	-0.9	2073.	2072.4
	0 1 0 0 0 1	2660.6	-0.4	2661.	2660.7
	0 0 0 0 1 0	3620.1	0.1	3620.	3618.8
	0 0 0 1 1 0	3978.7	0.1	3978.6	3977.1
RMS		–	0.115	–	–
RMS to observed		1.473	–	1.391	–

TABLE VIII. Comparatif entre le calcul de référence et les valeurs de Malyszek et Koput[108] et à celles observées. Les différences sont calculées par rapport aux valeurs de Malyszek et Koput[108]. Les deux dernières lignes représentent resp. les RMS des différences par rapport à Malyszek et par rapport à l'expérience. Les valeurs observées sont extraites de[123–127].